

Investigation Into Adaptive Slicing Methodologies for Additive Manufacturing

By

Qinkai Yang

Thesis submitted to Imperial College London
for the Degree of Master of Philosophy
and Diploma of Imperial College London

September 2021

Supervised by Dr Connor Myant and Dr Nan Li

Advanced Manufacturing Group
Dyson School of Design Engineering
Imperial College London

Declaration

I, Qinkai Yang, declare the work presented in this thesis is my own and that it is the one that will be used to be examined.

Copyright

The copyright of this thesis rests with the author and is made available under a Creative Commons Attribution Non-Commercial No Derivatives licence. Researchers are free to copy, distribute or transmit the thesis on the condition that they attribute it, that they do not use it for commercial purposes and that they do not alter, transform or build upon it. For any reuse or redistribution, researchers must make clear to others the licence terms of this work.

Abstract

Adaptive slicing is a methodology used to optimise the trade-off between build-time reduction and geometric accuracy improvement in additive manufacturing (AM). It works by varying decreasing layer thickness in sections of high curvature. However, current adaptive slicing methodologies all face the difficulty of adjusting layer thickness precisely according to the variations of the model's geometry, thereby limiting the geometric accuracy improvement.

This thesis tackles this difficulty by indicating the geometric variations of the model by evaluating the ratio of the volume of each sliced layer's geometric deviation to the volume of its corresponding region in the digital model. This indication is accomplished because all the topological information of the corresponding region is considered in assessing the geometric deviation (volume) between each sliced layer and its corresponding region. Through having this precise indication to modify each layer thickness, this thesis aims to develop an adaptive slicing that can mitigate geometric inaccuracies (e.g. staircase effect and dimensional deviation) while balancing the build time. This slicing is evaluated using six different test models, compared with three current slicing methodologies (voxelisation-based, cusp height-based, and uniform slicing), and validated through computation and manufacturing. These validations all demonstrate that volume deviation-based slicing optimises the trade-off between build-time reduction and geometric accuracy improvement better than the other existing slicing methodologies. For example, it can reduce the build time by nearly half compared to other existing slicing methodologies assuming a similar degree of printed parts' geometric accuracy.

The improved trade-off optimised by volume deviation-based slicing can directly benefit the AM applications in the aerospace and medical industries. This is because current research has shown geometric inaccuracies are the primary cause of reducing energy efficiency (e.g. turbine blade and wind tunnel testing models) and having failed implants (e.g. hip and cranial implants, dental prostheses). In addition to improving the geometric accuracy of AM-constructed parts, volume deviation-based slicing may also be incorporated with non-planar layer slicing. Non-planar layer slicing is designed to mitigate the mechanical anisotropy of printed parts by using curved-sliced layers. By integrating volume deviation-based slicing with non-planar layer slicing, the thickness of each curved-sliced layer can be adjusted according to the model's geometric variations and, therefore, has a possibility of reducing the geometric inaccuracies and mechanical anisotropy simultaneously.

Contents

Chapter 1: Introduction.....	10
1.1. Research Questions	12
1.2. Structure of Thesis.....	12
Chapter 2: A Critical Review of Current Slicing Methodologies	13
2.1. Uniform Slicing.....	14
2.2. Adaptive Slicing	14
2.2.1. Adaptive Slicing Based on Commonly Used Geometric Error Measurement..	15
2.2.2. Adaptive Slicing Based on 3D Geometric Error Measurement	17
2.2.3. Limitations of Adaptive Slicing Procedure	19
2.3. Non-Planar Layer Slicing	19
2.4. Conclusions	20
Chapter 3: Experimental Methods.....	22
3.1. Volume Deviation-Based Slicing	23
3.1.1. Initial Slicing.....	23
3.1.2. Evaluating the Volume Deviation of a Sliced Layer	24
3.1.3. Adjusting the Preliminary Layer Thickness.....	26
3.2. Experimental Methods	27
3.2.1. Computational Validations	27
3.2.2. Manufacturing Validations.....	28
Chapter 4: Computational Validations	32
4.1. Performance Tests of Volume Deviation-Based Slicing Methodology	33
4.1.1. Fixed build time effect on geometric accuracy.....	33
4.1.2. Fixed geometric accuracy effect on build time.....	37

4.2. Evaluating the Fairness of Comparison.....	39
4.3. Conclusions on Computational Validations	42
Chapter 5: Manufacturing Validations	43
5.1. Manufacturing Results and Discussions.....	44
5.2. Conclusions on Manufacturing Validations.....	48
Chapter 6: Conclusions and Suggestions for Future Works	50
References	53

List of Tables

Chapter 3

<i>Table 1. The predefined connectivity lists used for different surfaces.....</i>	<i>25</i>
<i>Table 2. Experimental test specimens and their number of sliced layers.....</i>	<i>27</i>
<i>Table 3. Main print settings applied to the slicer.....</i>	<i>30</i>

Chapter 4

<i>Table 4. The number of sliced layers generated by slicing methodologies when the printed part's geometric accuracy is limited to a similar layer degree</i>	<i>38</i>
--	-----------

List of Figures

Chapter 1

Figure 1. An illustration of staircase effect (circled by red-rectangle) and dimensional deviation (circled by orange-rectangle) induced by slicing in a printed part. Blue rectangles indicate the stack of sliced layers, dark-solid lines represent the slices, and the dark-dash line is the digital model's 2D profile. 12

Chapter 2

Figure 2. An illustration of the cusp height between a (3D) sliced layer (dark-blue cylinder) and its corresponding region (e.g. red mesh) in the triangulated surface model; the light-blue circle indicates the (2D) slice of each sliced layer. 15

Figure 3. (a) A curved beam sliced using planar layer slicing, (b) A curved beam sliced using non-planar layer slicing [34] 20

Chapter 3

Figure 4. Flowchart of volume deviation-based adaptive slicing methodology (the three main processes to determine each layer thickness are highlighted in blue) 23

Figure 5. A schematic overview of evaluating the volume deviation of a sliced layer..... 24

Figure 6. Procedure of detecting printed parts' profile for evaluation. (a) Raw image, (c) convert the truecolor image into a binary image and segment the printed part from this image, (d) edge detection. 30

Chapter 4

Figure 7. Sliced layers' maximum, mean, and minimum VD induced by slicing Test Models 1–6 using volume deviation-based (blue circle), voxelisation-based (green right-pointing triangle), cusp height-based (back cross) and uniform slicing (upward-pointing yellow triangle for slicing with the same number of layers and red square for slicing with minimum machine-allowable thickness). The sliced layers' maximum VD of uniform (thinnest) slicing on Test Model 3 and voxelisation-based slicing on Test Models 1, 4, and 5, which do not plot on the figure for clarity, are 9.7, 2.6, 2.9, and 3.4, respectively. 33

Figure 8. The colourmap of each stack of sliced layers generated by volume deviation-based, voxelisation-based, cusp height-based, and uniform slicing, respectively..... 35

Figure 9. The sliced layer (red) caused a sizeable volume deviation ratio (9.7 VD) from its corresponding region (yellow) in Test Model 4. 36

Figure 10. Sliced layers' VD induced by slicing Test Models 1 and 4 using volume deviation-based (blue), voxelisation-based (green), cusp height-based (grey) and uniform slicing (yellow); the number of sliced layer for each stack of sliced layers generated by these slicing methodologies is summarised in Table 4 38

Figure 11. Colourmap of each stack of sliced layers generated by voxelisation-based slicing before and after voxelisation resolution improvement. Scale: 1 indicates slicing using the original models' size and machine-allowable thickness, while 15 refers to slicing by enlarging the models' size and allowable thickness by 1,500%. The zoom-in areas in each stack of sliced layers are the critical regions (small volume sections with a high surface curvature and geometric complexity) of the Test Models. The slices of Test Models 4 and 6 are not shown on the figure for clarity..... 40

Figure 12. Colourmap of each stack of sliced layers generated by volume deviation-based slicing; these sliced layers were generated with the original models' size (scale 1) and machine-allowable thickness..... 40

Chapter 5

Figure 13. The deviation (blue area) between the 2D designed shape (dashed line) of Test Model 2 and the profile (solid line) of the parts, which were printed by using volume-deviation based (a), voxelisation-based (b), and uniform slicing (c). The bar graph next (right) to each profile analysis presents the area of the discrepancy between each fabricated layer contour and its corresponding region shape; the Y-axis of each bar element indicates the layer

number (from 2nd to 56th), while the X-axis represents the discrepancy area (cm²). For results clarity, the discrepancy in the first layer is not shown. This layer has a risk of warping due to thermal stress caused by uneven heat distribution and has a high risk of a slight shape distortion incurred by the operator when removing the printed part from the build platform. These risks may affect the analysis accuracy of evaluating the geometric inaccuracies of printed parts induced by only the slicing..... 45

Figure 14. The deviation (blue area) between the 2D designed shape (dashed line) of Test Model 4 and the profile (solid line) of the parts, which were printed by using volume-deviation based (a), voxelisation-based (b), and uniform slicing (c). The bar chart next (right) to each profile analysis shows the area of the discrepancy between each fabricated layer contour and its corresponding region shape; the Y-axis of each bar element indicates the layer number (2nd to 115th), while the X-axis represents the discrepancy area (cm²). For results clarity, the discrepancy in the first layer is not shown. 46

Figure 15. (a) The thickness of each sliced layer produced by volume deviation-based (blue circle) and voxelisation-based slicing (green right-pointing triangle) for Test Model 2 against the layer number. The shape of the last layer of the part printed by using volume deviation-based slicing during (b) and after (c) fabricating this layer..... 48

Acknowledgements

I would like to express my gratitude to my supervisor, Dr Connor Myant, for his inspiration and advice throughout the project.

Special thanks to Prof. Dr. Marc Alexa at Berlin Institute of Technology and Sylvain Lefebvre at INRIA for their kindness in sharing the information (test specimens, voxel size, and slicer) related to their voxelisation-based slicing.

Huge thanks are given to my family for their support and accompany, especially during the COVID lockdown period when I was living alone for more than seven months. They are always there when I need a call.

Chapter 1: Introduction

This chapter provides the background and motivations of this project. It then states the aim and research questions that this thesis is targeting. Finally, it outlines the structure of this dissertation.

Additive manufacturing (AM), also known as 3D printing, is defined as a process of joining materials to create objects from 3D model data, usually by placing planar layer upon planar layer [1]. Most current AM technologies share a common information flow, the 'digital thread', to define the fabrication path [2,3]. This digital thread begins with the creation of a 3D model in a Computer-Aided Design (CAD) package and ends with the printed object. In this digital thread, slicing is a vital step. Slicing can be defined as a digital process by which a triangulated surface model is replaced by a stack of discrete (2D) slices containing the model's perimeter information. Each slice and its perpendicular projection on the previous adjacent slice (the first slice is projected on the machine build plane) define the shape of the top and bottom surfaces of a (3D) sliced layer of an AM-fabricated part. These layers are typically spaced uniformly and often set by the user via the layer thickness parameter. While this projection of each layer onto the next is a practical and straightforward approach for defining the layers of constructing printed parts, it inadvertently leads to geometric inaccuracies.

The geometric inaccuracies occur because the CAD model's original curved contours are reduced to a monotonic stepwise topography set up by the layer thickness, resulting in staircase effect in printed parts, as shown in Figure 1. In addition to the staircase effect, a dimensional deviation (Figure 1) can also result when the CAD model's geometric feature is not located between two adjacent layers [4]. These two common slicing-induced geometric inaccuracies are directly affected by the layer thickness parameters and significantly limit the potential of additive manufacturing in the current industry. For example, using AM to construct wind tunnel testing models, printed parts with a higher staircase effect induce a higher axial force coefficient than the model's desired shape [5–7]. In turbine blade application, dimensional accuracy is critical for energy efficiency and vibration reduction [8,9]. In using AM in investment casting for biomedical implants, the poor geometric accuracy of printed parts (moulds) is further inherited by castings, resulting in failed implantation [10–13].

To address these geometric inaccuracies, current industries frequently apply post-processing for surface treatment after the parts have been fabricated by the AM machine [14–21]. Post-processing usually refers to smoothing the peaks of the surface profiles of printed parts mechanically or chemically [11,19]. While this process can mitigate the staircase effect, it can also result in a further dimensional deviation in the printed part due to material subtraction or addition. Besides increasing dimensional deviation, post-processing can amount to 24.68% of the total production cost of an AM-fabricated part and represent approximately 46% of total manufacturing time [22–24]. To reduce the need for post-

processing and mitigate geometric inaccuracies, a better slicing methodology that can result in the profile of the part coming closer to its designed shape is desired by industries.

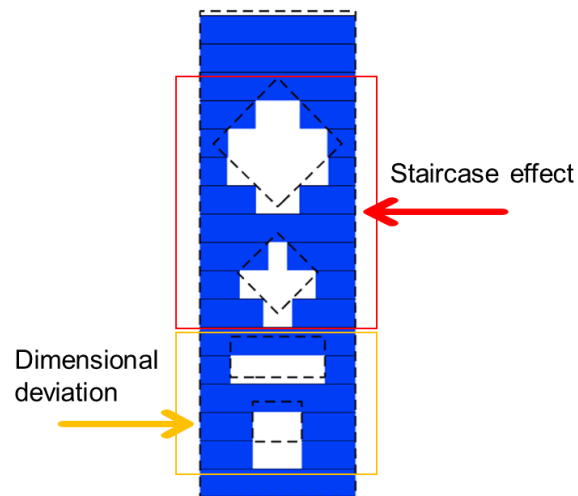


Figure 1. An illustration of staircase effect (circled by red-rectangle) and dimensional deviation (circled by orange-rectangle) induced by slicing in a printed part. Blue rectangles indicate the stack of sliced layers, dark-solid lines represent the slices, and the dark-dash line is the digital model's 2D profile.

1.1. Research Questions

This project plans to answer the following research questions:

1. How can both the staircase effect and dimensional deviation of printed parts be mitigated while balancing the build time?
2. What degree of mitigation can result from these modifications, compared to existing slicing methodologies?

1.2. Structure of Thesis

The thesis starts with a literature review of current slicing methodologies in chapter 2.

Chapter 3 centres on introducing the proposed slicing methodology. This is volume deviation-based slicing, which adjusts each layer thickness based on the ratio of the volume of each sliced layer's geometric error to the volume of its corresponding region in the digital model. This chapter then describes the experimental methods and equipment used for validating and implementing volume deviation-based slicing in computation and manufacturing.

Results obtained from computational and manufacturing validation are presented and discussed in chapters 4 and 5, respectively.

Finally, conclusions, possible limitations, and future works on this research project are given in chapter 6.

Chapter 2: A Critical Review of Current Slicing Methodologies

The following chapter provides a detailed review of the current slicing methodologies, which can be primarily classified into three groups: uniform slicing, adaptive slicing, and non-planar layer slicing. Particular reference is given to the slicing used to optimise the trade-off between build-time reduction and geometric accuracy improvement.

2.1. Uniform Slicing

Uniform slicing, which generates sliced layers with uniform thickness, is the most widely used slicing methodology in the current industry. Its wide acceptability maybe because it is easy to operate, as its only user-defined parameter is layer thickness. While uniform slicing has this advantage, because of this lack of parameters that can be used to control its slicing process, it has difficulty in addressing the staircase effect and dimensional deviations. To mitigate these geometric inaccuracies, a great deal of work has been done to investigate the relationship between part's geometric accuracy and layer thickness selections.

Lanzotti et al. [25] investigated the dimensional accuracy of printed parts constructed differently with the layer thickness of 0.10, 0.15, and 0.20 mm. Paul and Voorakarnam [26] used the layer thicknesses of 0.112 and 0.224 mm to evaluate the staircase effect of the parts, fabricated from these thicknesses. García-Plaza et al. [27] analysed the dimensional (length, width, and height) deviation and surface texture of parts built separately with the layer thicknesses of 0.06, 0.12, 0.18, and 0.24 mm. Similar research for studying the relationship between a part's geometric accuracy and layer thickness choices was also conducted in [28–30]. Although different layer thicknesses were chosen in these investigations, research all agreed that thinner layers result in smaller geometric inaccuracies, particularly the staircase effect. The printed part's staircase effect is mitigated because its monotonic stepwise topography, which is set up by the layer thickness, converges closer to the designed shape by minimising the layer thickness.

However, minimising the layer thickness does not always guarantee an improvement in dimensional accuracy, as the optimal thickness used for uniform slicing to capture the geometric feature of a part may vary from feature to feature. Thus, the dimensional deviation remains when a geometric feature, such as a peak or flat area, is not located between two adjacent layers with minimum thickness [4]. In addition to this limitation, minimising the layer thickness can also incur a longer build time as the number of layers increases. To combat this build time penalty for increasing geometric accuracy and to vary layer thickness according to the model's geometry, adaptive slicing methodologies have been proposed.

2.2. Adaptive Slicing

Adaptive slicing sought to optimise the trade-off between build time and geometric accuracy by varying decreasing layer thickness in sections of high curvature. It determines each layer thickness by evaluating the geometric deviation between each constructed (planar) sliced layer and a corresponding region in the digital model, as shown in Figure 2. In reducing the

geometric error of each sliced layer within a user-specified tolerance by decreasing the layer thickness, the staircase effect of the printed parts is mitigated. A few studies have been conducted to develop adaptive slicing. However, most of these studies lack reliable validations for their slicing and face the challenge of accurately adjusting layer thickness according to the model's geometry.

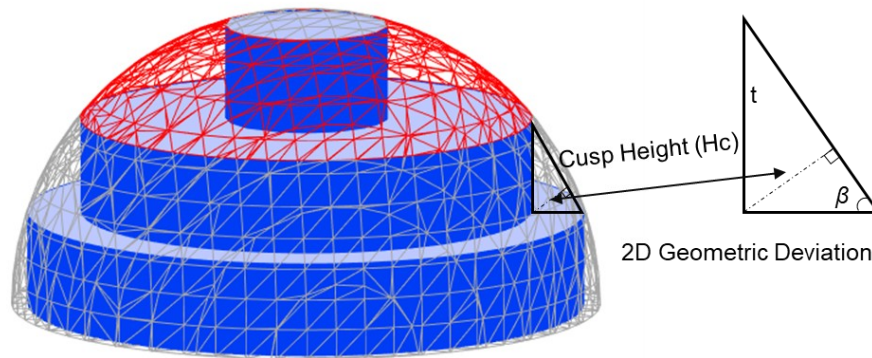


Figure 2. An illustration of the cusp height between a (3D) sliced layer (dark-blue cylinder) and its corresponding region (e.g. red mesh) in the triangulated surface model; the light-blue circle indicates the (2D) slice of each sliced layer.

2.2.1. Adaptive Slicing Based on Commonly Used Geometric Error Measurement

Cusp height and area deviation are typically employed to measure the geometric error of (planar) sliced layers [31–33]. However, these measurements do not result in an accurate evaluation of the geometric error, constricting the accuracy of layer thickness modification in adaptive slicing.

Cusp height is defined as the maximum distance between the surface of a sliced layer and its corresponding region in the triangulated surface. It is broadly applied in adaptive slicing methodologies [31,34–36], and is widely employed in commercial slicers (e.g. Slicer3r, PrusaSlicer, and Ultimaker Cura). Mao et al. [31] employed cusp height for evaluating the geometric deviation of sliced layers to adjust layer thickness; and found that cusp height-based slicing results in better geometric accuracy than uniform slicing. However, Mao et al. compared their slicing with uniform slicing by evaluating the maximum cusp height among all layers sliced by these two slicing methodologies and visually judging the surface finish of specific areas of the printed parts from microscope images. In these comparisons, the number of sliced layers generated by these two slicing methodologies was not the same. Thus, the slicing of Mao et al., which produced more layers than uniform slicing in comparisons, naturally resulted in a more negligible staircase effect, affecting their experiment reliability.

Danjou and Köhler [36] also investigated the slicing performance of cusp height-based slicing and uniform slicing by visually comparing the sliced layers produced by these slicing methodologies in digital models. Sliced layers produced by cusp height-based slicing were limited to be less than those created by uniform slicing in [36]. By limiting the number of sliced layers, they identified that cusp height-based slicing outperformed uniform slicing in optimising the trade-off between build-time reduction and geometric accuracy improvement. This statement was made because cusp height-based slicing can produce more layers in some sections with high curvature in the digital model compared to uniform slicing.

Although the above research all agreed that cusp height-based slicing was better than uniform slicing, the reliability of these conclusions may need to be further verified, as these studies mainly relied on subjective–visual evaluations. While there is a lack of research for accurately analysing the benefits of applying cusp height in adaptive slicing, several drawbacks of using cusp height to measure sliced layers' geometric deviation can be clearly identified. Cusp height can induce approximate error, causing slicing to produce sliced layers that are inconsistent with the model's geometric complexity. This error happens because, for sliced layers with the same cusp height, the areas of the (2D) geometric deviations between these layers and their corresponding regions can differ. This approximate error can be aggravated, particularly with regard to the sliced layers in the model's flat areas.

To overcome this approximate error in measuring the geometric deviation of sliced layers in flat areas, Yang et al. [37] proposed using the deviation between the areas of the top and bottom slices of a sliced layer to measure its geometric error. By employing this area deviation measurement, their slicing produced thinner sliced layers around the model's flat areas than cusp height-based slicing. While these thin layers may mitigate the geometric deviations in these areas, no quantitative comparison was conducted by Yang et al. to investigate the geometric accuracy reached by their slicing and other slicing methodologies.

Similar to Yang et al., Zhao et al. [38] also proposed an area deviation-based slicing. Within the same limitation of a user-defined tolerance (maximum area deviation), a model that was sliced using area deviation-based slicing exhibited approximately 94% fewer layers than when it was sliced through uniform slicing. However, this considerable layer reduction was because the sliced layers produced by uniform slicing was 30 times thinner than the thickest layers created by area deviation-based slicing, and the test specimen had half of its section in low surface curvature. Zhao et al. have also not validated the accuracy of using area deviation to evaluate the geometric error of sliced layers or compared this slicing with other adaptive slicing methodologies. Although lacking validations, Fu et al. [39] and Rianmora et al. [40] still clearly identified the main limitation of area deviation. This limitation is that the topological information within the corresponding region of a sliced layer may not be captured

using area deviation, particularly if the areas of a sliced layer's top and bottom slices are the same.

In addition to inducing approximate error (cusp height) and ignoring topological information (area deviation), these two measurements in commonly used adaptive slicing approach a sliced layer's geometric error as a 2D error (considering the geometric error's shape as a polygon). This 2D error was used to indicate the surface curvature of the sliced layer's corresponding region for the layer thickness adjustment. By approximating geometric deviation as a 2D error, the evaluated results can vary when these measurements are used to assess the geometric error from different orientations of a sliced layer. This issue limits the accuracy of adaptive slicing modifying each layer thickness according to models' surface curvature; this limited accuracy then restricts adaptive slicing in mitigating staircase effect. By only indicating surface curvature changes, these measurement methods cannot differentiate the complexity of a model's geometric features, such as vertical, peak, and flat areas. This problem constrains adaptive slicing's performance in generating sliced layers representing these geometric features, thereby inducing dimensional deviations.

2.2.2. Adaptive Slicing Based on 3D Geometric Error Measurement

A sliced layer's geometric deviation is affected by both the topological information of its corresponding region and its layer thickness, as shown in Figure 2. Thus, by assessing this geometric deviation's volume, there is a possibility of capturing all the topological information of the corresponding region, which can indicate both the variations of the surface curvature and geometric complexity. A few studies have tried to realise this possibility in their slicing methodologies by measuring the geometric error of sliced layers as a 3D geometric error.

Kumar et al. [41] intended to calculate the volume variation between each sliced layer and its corresponding region in the CAD model. They represented each sliced layer by simplifying its corresponding region into a coarse quadrilateral mesh. The volumetric error in the research conducted by Kumar et al. was then calculated as the volume deviation between the quadrilateral mesh of a sliced layer and the corresponding region of this layer in the CAD surface. By calculating this deviation, Kumar et al. claimed that their measurement could potentially indicate the topological information of sharp edges in the model. However, no experiment was conducted to validate this potential of the measurement method or the performance of this measurement-based slicing. In addition to the lack of validations in [41], by calculating the volume deviation between the quadrilateral mesh of sliced layer's corresponding region and the CAD surface, Kumar et al. ended up calculating a sliced layer's geometric deviation as a 3D chordal error.

Taufik et al. [42] attempted to calculate the volume discrepancy between the sliced layer and a corresponding region in the triangulated surface model using the sliced layer's area deviation to multiply half of its layer thickness. They stated that this measurement could accurately examine sliced layers' geometric deviation; the measured volumetric error in their experiments constantly varies with the surface curvature of sliced layers' corresponding regions. In addition to a model with a simple geometric form was chosen in these experiments, multiplying area deviation with half layer thickness indicated that the shape of a sliced layer's geometric deviation approximates that of a triangular prism. Despite this approximate error, the limitations of the area deviation discussed above can also cause this measurement method [42] to ignore the topological information in the sliced layer's corresponding region. Taufik et al. also applied this measurement in adaptive slicing for layer thickness modifications. However, no experiment was done for validating their slicing's performance.

Alexa et al. [43] voxelised a sliced layer and its digital model's corresponding region, calculating the volume deviation of the sliced layer by counting the number of non-intersected voxels between the two voxelised objects. By using this voxelisation method to measure the sliced layer's geometric deviation, voxelisation-based slicing produced a better trade-off between build-time reduction and geometric inaccuracy mitigation than uniform and cusp height-based slicing. This comparison result was obtained by Alexa et al. through qualitative and quantitative analysis. In qualitative experiments, similar to the validation issues discussed in [31], Alexa et al. visually judged the sliced layers in the digital model and the surface finish of printed parts' specific areas from microscope images. In quantitative experiments, Alexa et al. compared voxelisation-based slicing with uniform and cusp height-based slicing by assessing how these three methodologies preserved the model's mass within the limitation of the same number of sliced layers. Although using both the quantitative and qualitative analysis for verifications increases their conclusion's reliability, their quantitative analysis was conducted inaccurately. This quantitative analysis is inaccurate because the total volume discrepancy between a printed part and its digital model does not directly relate to the printed part's geometric accuracy. A sliced layer in a model's large sections with low surface curvature will result in a more significant volume deviation than a sliced layer with the same thickness in the model's small sections with high surface curvature. This inconsistent variation between evaluation results and surface curvature limits the reliability of the conclusion for voxelisation-based slicing in [43]. Furthermore, because voxelisation approximates the geometric features of sliced layers and sliced layers' corresponding regions, an approximation is induced in assessing sliced layers' geometric deviation.

Taufik et al. [44], Sikder et al. [45], and Deng et al. [46] also considered the geometric deviation between a sliced layer and its corresponding region as a 3D geometric error in their adaptive slicing methodologies. However, none of these slicing methodologies has a measurement method that can accurately calculate the volume of each sliced layer's geometric deviation. This challenge of precisely assessing the sliced layer's geometric deviation further restricts adaptive slicing's performance in mitigating both the staircase effect and dimensional deviation of printed parts.

2.2.3. Limitations of Adaptive Slicing Procedure

Despite the constraint from measurement methods, in most of the adaptive slicing explored above, the alleviation of geometric inaccuracies has also been limited by its slicing procedure. This limitation happens because most of these slicing methodologies initially slice a digital model uniformly with either a maximum or minimum layer thickness restricted by the AM machine [32,45,47]. The geometric error of each sliced layer is evaluated, and when the evaluated geometric error of a sliced layer is outside the user-defined tolerance, the layer thickness is reduced.

However, initially slicing a digital model using uniform layer thickness also defines the number of sliced layers of the part that will be constructed. The height of a constructed part is determined by summing the thicknesses of its sliced layers. To maintain the desired fabricated height specified by the digital model, adjusting the thickness of a sliced layer requires a corresponding modification of the thicknesses of the other sliced layers. Therefore, the variation in each layer thickness is defined by the geometric error evaluation and is also affected by the number of sliced layers determined by the uniform slicing process.

Mao et al. [31] overcame this limitation by initially slicing a model into a stack of uniform intervals (temporary sliced layers); the distance between these intervals was smaller than the minimum thickness of the machine specifications. The geometric error of each interval was then evaluated using the cusp height. By joining these intervals until a sliced layer's cusp height reached the maximum user-defined tolerance or until the layer thickness reached the maximum machine-allowable thickness, the thickness of a sliced layer was defined. While this slicing procedure does not affect the layer thickness modification, it is computationally expensive.

2.3. Non-Planar Layer Slicing

In addition to geometric inaccuracies, mechanical anisotropy is unavoidable in AM-fabricated parts due to the recursive fusion process [48,49]. Thus, inconsistent load capacity of AM parts can occur when forces are applied from different directions, such as parallel to or

across layers [48]. Some researchers have noted that the shape of slices affects the anisotropic behaviour of AM-constructed parts by affecting their compressive and tensile strength [50–55]

Non-planar layer slicing, also known as curved-layer slicing, was first proposed by Chakraborty et al. [55] to mitigate the mechanical anisotropy of AM-fabricated parts. The aim of this slicing methodology was to manufacture slightly curved (shell-type) parts using non-planar (curved) layers. The slices of these curved-sliced layers were spaced uniformly and generated by offsetting the bottom (parametric) surface of a desired fabricated part's digital model along the positive Z-direction of this surface. By printing a slightly curved part based on these curved slices, a continuous filament structure can be achieved within, as shown in Figure 3 (a) and (b). Therefore, the contact area between each adjacent constructed layer is increased. This increased contact area reduces the mechanical anisotropy of the printed parts by strengthening the interlayer bonding [56–59].

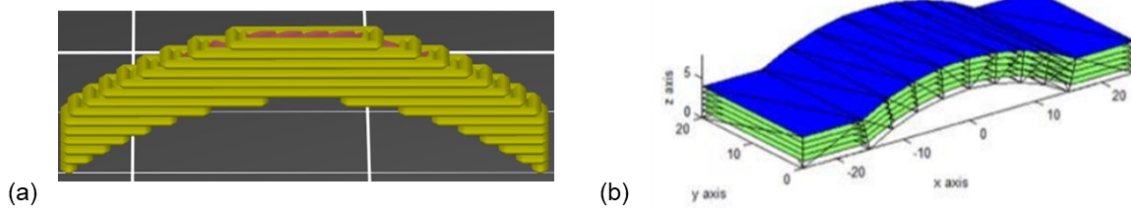


Figure 3. (a) A curved beam sliced using planar layer slicing, (b) A curved beam sliced using non-planar layer slicing [34 p.364]

Some researchers have also stated that non-planar layer slicing methodologies could partially eliminate the staircase effect of AM-constructed parts [51,52,55,60,61]. This elimination is due to curved slices being generated by offsetting either the top or bottom surface of a model. This slice generation enables the curved contour of these top or bottom surfaces to be represented in the curved-sliced layers. However, when using these curved-sliced layers to construct models with geometric features similar to a sphere, the staircase effect remains between each curved-sliced layer's infill. Isa and Lazoglu [62] argued that generating curved slices based on surface offsetting considers only the geometric features of offset surfaces and cannot mitigate the part's other bounding surfaces' staircase effect. Non-planar layer slicing also does not consider the models' geometric features in determining the thickness of each sliced layer; therefore, a high geometric deviation can be induced in sliced layers.

2.4. Conclusions

A review of the above-cited literature reveals the following limitations of the current slicing methodologies:

1. Although most research agreed that minimising layer thickness in uniform slicing reduces the staircase effect in AM-constructed parts, this action may not improve dimensional deviation and incurs a longer build time.
2. Most current adaptive slicing methodologies lack reliable validation to investigate their effectiveness in optimising the trade-off between build-time reduction and geometric accuracy improvement.
3. The layer thickness modification in the current adaptive slicing methodologies is limited by inaccurate measurements for the geometric deviation of sliced layers and is affected by their slicing procedures (adjusting each layer's thickness following uniform slicing).
4. A few studies suggested that non-planar slicing may mitigate printed parts' staircase effect because the curved-sliced layers can represent the curved contour of the digital model's top or bottom surfaces [51,52,55,60,61]. However, this mitigation is restricted by models' geometry, and this type of slicing can cause a high degree of geometric deviation in the sliced layers.

In conclusion, there is not yet a type of slicing that can accurately adjust each layer thickness according to the variations of the model's surface curvature and geometric complexity to mitigate both the staircase effect and dimensional deviation. Therefore, the primary focus of this research will be on developing a measurement method that can be employed in slicing methodologies to indicate both the variations of surface curvature and geometric complexity without inducing approximate error. By accurately assessing the model's geometric features, the developed adaptive slicing may accurately adjust each layer thickness according to the model's geometry. By having this type of layer thickness modification, the proposed adaptive slicing could outperform existing slicing methodologies in terms of optimising the trade-off between geometric accuracy (staircase effect and dimensional deviation) and build time.

Chapter 3: Experimental Methods

This chapter describes the volume deviation-based slicing proposed in this research and used to adjust each layer thickness following both the surface curvature and geometric complexity variations. Two experiments are planned to evaluate this slicing, using qualitative and quantitative analysis in both the computation and manufacturing verifications. Results from these verifications are presented in the subsequent chapter.

3.1. Volume Deviation-Based Slicing

Previous research modified the thickness of each sliced layer after uniform slicing, limiting the accuracy of the layer thickness adjustment. Therefore, in volume deviation-based slicing, the thickness of a sliced layer is only calculated and adjusted after the thickness of its previous adjacent layer is determined. The workflow (as shown in Figure 4) for determining each layer thickness is summarised as follows:

- 1) Initially slice an object driven by the inputted cusp height.
- 2) Evaluate volume deviation for each sliced layer.
- 3) Adjust layer thickness until its evaluated volume deviation ratio is within a user-specified tolerance.

The next sections explain how each layer thickness is defined as following this workflow.

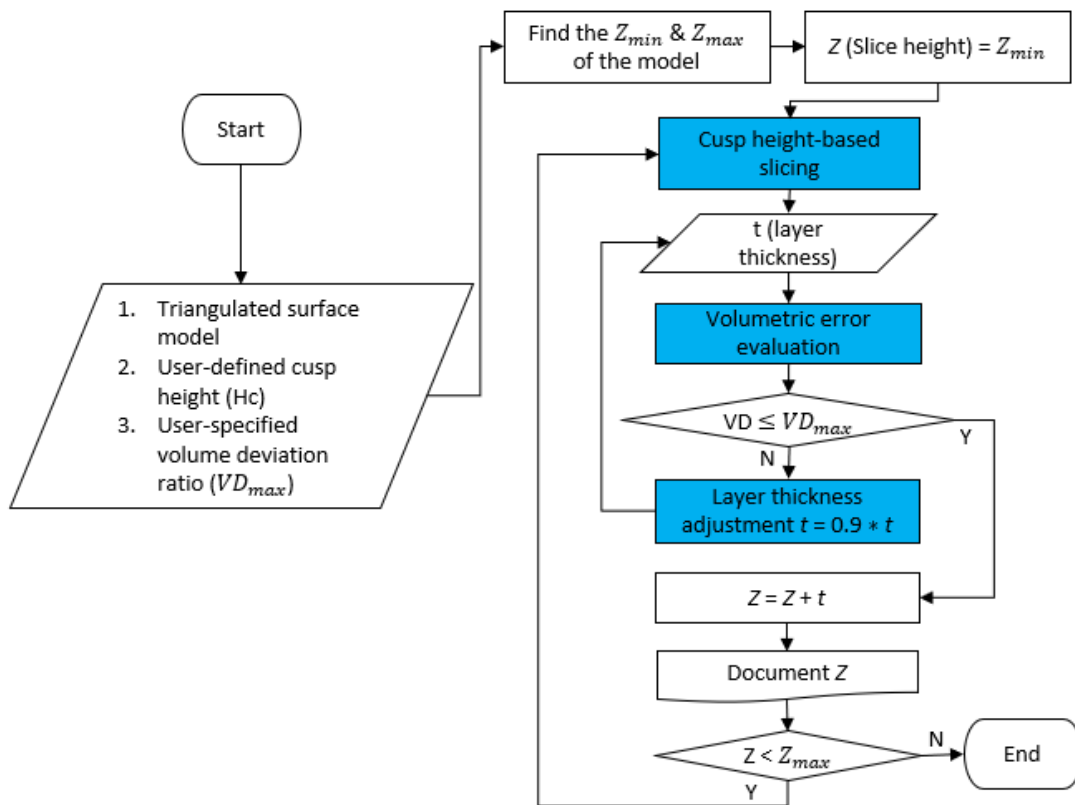


Figure 4. Flowchart of volume deviation-based adaptive slicing methodology (the three main processes to determine each layer thickness are highlighted in blue)

3.1.1. Initial Slicing

The cusp height is employed to calculate the preliminary layer thickness, $t_{preliminary}$. Applying cusp height to determine the preliminary layer thickness aims to reduce the difference between this thickness and the final layer thickness to reduce the iterative computation of volumetric error measurement and layer thickness adjustment in the workflow. Here $t_{preliminary}$ is calculated as follows [34,63]:

$$t_{preliminary} = \frac{Hc}{\cos \beta} \quad (1)$$

The cusp height, Hc , is specified by the user. Thus, only the surface angle, β , between the triangles in a sliced layer's corresponding region and the build plane (the print bed or a previous adjacent slice) needs to be defined. β can be calculated as:

$$\cos \beta = \left| \frac{n \cdot [0 \ 0 \ 1]}{\|n\| \cdot \|[0 \ 0 \ 1]\|} \right| \quad (1)$$

where, n is the unit normal vector of a triangular facet, and $[0 \ 0 \ 1]$ is an auxiliary vector pointing along the positive build direction.

Due to the sliced layer's corresponding region featuring many triangles, the β of the triangles intersecting with the build plane are then averaged to define the preliminary layer thickness $t_{preliminary}$ ($t_{min} \leq t_{preliminary} \leq t_{max}$, where t_{min} and t_{max} are respectively the minimum and maximum layer thickness constrained by the AM machine).

3.1.2. Evaluating the Volume Deviation of a Sliced Layer

Evaluating the volume deviation of a sliced layer consists of three main steps (shown in Figure 5). Step 1 involves constructing two manifold triangular meshes representing the sliced layer and its corresponding region in a digital model. Step 2 entails generating a triangulated surface to represent the intersection between these two meshes. Step 3 requires calculating the volume discrepancy between the constructed sliced layer and its corresponding region; this is achieved by using the volumes of the sliced layer and its corresponding region to subtract their intersection volume, respectively.

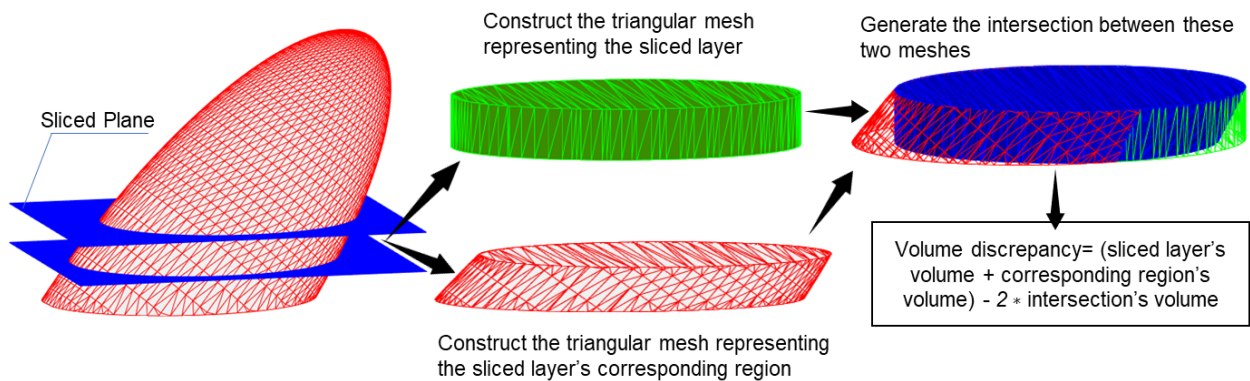


Figure 5. A schematic overview of evaluating the volume deviation of a sliced layer

First, the triangular meshes of a sliced layer's two slices are constructed. To construct these meshes, two horizontal planes with Z heights equal to the Z height of the sliced layer's top and bottom slices are used to intersect the digital model. A plane-line intersection algorithm is then used to identify the intersection points between the sides of each triangular facet in

the digital model and these two planes [64]. If a side intersects with a plane at a single point, this algorithm identifies this intersection point by calculating a scalar for multiplying a vector representing this side. By extracting the intersection points and subsequently conducting the MATLAB *polyshape* function for the intersection points in each plane, the polygons of the top and bottom slices of the sliced layer are created. These polygons are then represented separately by a triangular mesh using the MATLAB *triangulation* function.

Next, the triangular meshes are enclosed by filling a perimeter surface to produce a complete manifold triangulated surface of the sliced layer's corresponding region. The perimeter surface is defined by the triangles in the region where the sliced layer is located in the digital model. In this region, the triangular facets that intersect with the slices can be broken. These broken triangles need repairing to form a complete triangulated mesh. Each broken triangle's vertices are the intersection points between this triangle and slices, and the vertices of this intersected triangle in this region. By extracting the vertices of each incomplete triangle and applying three predefined connectivity lists (as presented in Table 1) to specify the connections among these vertices, each broken triangle's surface can be defined by a set of triangular facets. The construction of these lists follows the data format in MATLAB triangulation function and is based on identifying that there are only three types of broken triangle surfaces; triangle, quadrilateral, and pentagon.

Table 1. The predefined connectivity lists used for different surfaces

Types of Surface	Triangle	Quadrilateral	Pentagon
Examples			
Predefined Connectivity List	$[1 \ 2 \ 3]$	$\begin{bmatrix} 1 & 2 & 3 \\ 1 & 3 & 4 \end{bmatrix}$	$\begin{bmatrix} 1 & 2 & 3 \\ 1 & 3 & 4 \\ 1 & 4 & 5 \end{bmatrix}$

After constructing the manifold triangulated surface of a sliced layer's corresponding region, a manifold triangular mesh representing the sliced layer is needed to be formed. The mesh of the sliced layer's top slice and the projection of this mesh in the bottom sliced plane define the top and bottom surfaces of the manifold triangular mesh of the sliced layer. To enclose this manifold triangular mesh's top and bottom surfaces by generating its perimeter surface, every two adjacent points on its top surface and the projection of these two points on the bottom surface are extracted. Subsequently, the facet defined by these four points is triangulated using the above predefined connectivity lists.

After forming these two manifold triangulated surfaces, a mesh intersection algorithm [65] is employed to construct a triangular mesh representing the intersection between these two triangulated surfaces. This algorithm first generates the intersection points between these two triangulated surfaces. These points can be calculated using the above plane-line intersection algorithm. The intersection points in each intersected triangle are connected to form intersection edges. The intersection edges in each intersected triangle are then used in edge-constraint triangulation [66] to create a set of triangular facets for representing this intersected triangle, as a triangle is broken by intersecting meshes. By repairing each broken triangle and identifying the triangles located in the intersection between the two triangulated surfaces, an intersection triangular mesh is formed.

Next, the volume, V_{sliced} , V_{region} , $V_{intersection}$, enclosed by the manifold triangulated surfaces of the sliced layer, the sliced layer's corresponding region, and the intersection, respectively, is calculated using the divergence theorem [67]. This theorem represents the flux of a vector field across a surface boundary, and can be stated as follows;

$$V = \iint_S Z \cdot N_z dS \quad (2)$$

Here, the flux of the vector field is constructed by the z-component, Z , of the barycentre position vector of each triangle in a triangulated surface, dS is the area of a triangular facet, N_z is the Z-component of that facet's normal vector, and $Z \cdot N_z dS$ indicates the total flux through that facet. The reason for only considering the vectors along Z-axis is that the model's volume is calculated as the same in the divergence theorem when the flux flows along each axis.

Thus, the volume deviation, $V_{deviation}$, can be found using;

$$V_{deviation} = (V_{sliced} - V_{intersection}) + (V_{region} - V_{intersection}) \quad (3)$$

3.1.3. Adjusting the Preliminary Layer Thickness

To adjust $t_{preliminary}$, a volume deviation ratio $VD = V_{deviation}/V_{region}$ is designed for the user to specify the maximum tolerance, VD_{max} , of the sliced layers' geometric error. The layer thickness, t ($t_{min} \leq t \leq t_{max}$), is determined when the VD of this sliced layer is within the user-specified tolerance, VD_{max} . If $VD > VD_{max}$, t is defined by iteratively reducing $t_{preliminary}$ with an interval of distance $itv = 0.1 * t_{preliminary}$ until $VD \leq VD_{max}$. 0.1 was chosen to limit the interval distance for reducing at each iteration, avoiding the VD of the adjusted layer thickness that is considerably smaller than VD_{max} .





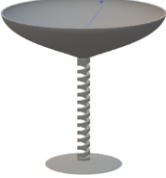

3.2. Experimental Methods

The experiments planned here aim to evaluate the performance of volume deviation-based slicing in optimising the trade-off between geometric inaccuracy (staircase effect and dimensional deviation) mitigation and build-time reduction. These evaluations will examine the geometric accuracy of digital and physical printed parts produced by volume deviation-based slicing, respectively, in computation and manufacturing.

3.2.1. Computational Validations

Volume deviation-based slicing will be tested on six specimens, representing a range of geometric forms from simple to complex, as summarised in Table 2. Its attained geometric accuracy in each test model will be compared with those achieved by three current slicing methodologies (voxelisation-based [43], cusp height-based, and uniform slicing). The sliced layers produced by these four slicing methodologies in the same specimen will be limited within the same limitation of the number of sliced layers and varied under the same range of machine-allowable thickness ($t_{min} = 0.05$ mm, $t_{max} = 0.3$ mm). Uniform slicing with the minimum machine-allowable thickness (Uniform (thinnest) slicing) will also be employed to evaluate the difference between the geometric accuracy achieved by volume-deviation based slicing and by using the optimal setting in current slicing. The slices of voxelisation-based slicing will be extracted from the G-code file produced by the commercial IceSL slicer [68] developed based on this adaptive slicing [43], while the other three slicing methodologies are implemented in MATLAB.

Table 2. Experimental test specimens and their number of sliced layers

Model Number	1	2	3	4	5	6
Model						
Model Height (mm)	6.00	11.50	16.60	27.55	27	16.41
Number of Sliced Layers	70	56	75	115	202	234
Number of Sliced Layers for Uniform (Thinnest) Slicing	120	240	331	550	540	328

* Test Model 1 was designed with surface curvature and geometric complexity variations (where are the sections that staircase effect and dimensional deviation frequently occur) mainly in its diamond-shaped and rectangular cavities. From Test Models 2 to 6, the complexity of models' geometric forms continually increases; these models contain the geometric features of symmetry, non-symmetry, and flat areas. Test Model 6 is the original test specimen used in the research of voxelisation-based slicing developments [43: p.13].

The geometric inaccuracies of a printed part produced by each slicing will be assessed quantitatively by looking at the sliced layers' volume deviation ratio. The indication of the volume deviation ratio on the staircase effect and dimensional deviation will be demonstrated by investigating the sections of occurring high volume deviation ratio and these two geometric inaccuracies in the printed parts of Test Model 1. Focusing solely on Test Model 1 is because of its simple geometric form; therefore, staircase effect and dimensional (height) deviation induced by the sliced layers can be respectively shown clearly in its diamond-shaped and rectangular cavities.

The experiments designed above has a potential limitation caused by generating the slices of voxelisation-based slicing using the IceSL slicer [68]. This slicer uses a voxel size of 0.25x0.25x0.0025 mm for slicing, while a voxel size of 0.05x0.05x0.001875 mm was employed in the original paper [43]. The larger voxel size that was applied in the slicer is its default voxel size and cannot be modified. Therefore, the influence of voxelisation resolution on the geometric inaccuracies of the printed part constructed using voxelisation-based slicing will be analysed to validate the fairness of the comparison between this slicing and volume deviation-based slicing's performance.

3.2.2. Manufacturing Validations

The aim is to validate whether the geometric accuracy accomplished by volume deviation-based slicing in digital printed parts can be transferred to physical fabricated parts and to explain how to implement this slicing on the machine. Volume deviation-based slicing will be compared to voxelisation-based and uniform slicing to differentiate their slicing performances again. Test Models 2 and 4 will be employed to examine the slicing performance in adjusting each layer thickness according to surface curvature variations and geometric complexity variations, respectively.

a) Slicer developments

The slices of these models, produced in computation validation by the three slicing methodologies, will be processed in a slicer to generate the AM machine manufacturing toolpath (wall, infill, and support structure (if overhanging features exist)).

- The wall toolpath is generated by using the MATLAB *polybuffer* function, which works here by buffering the data points in each slice by a user-specified distance.
- To produce the infill toolpath for a slice, initially, a set of lines with the same Z-height as the slice's is generated across the area of the machine's build platform. These lines are spaced from each other at a user-defined distance and oriented at a user-

specified angle to the platform longitudinal axis. The lines encompassed by the area of walls are then extracted using the *intersect* function.

- To structure the support toolpath, a triangulated surface model's overhanging features need to be identified first. These overhanging features are the triangles that face downward and are oriented to the build platform at an angle smaller than the user-defined build angle. These overhanging triangles are detected based on their normal vectors. The vertices of each overhanging triangle are then projected into the planes of the slices below this triangle. The projected vertices in each slice plane are enclosed by the boundary of a polygon created using the *boundary* and *polyshape* functions. Each polygon is then subtracted by the shape of its corresponding slice using the *subtract* function to form the boundary of the support toolpath at the same Z-height as this slice's. By generating the infill in these boundaries, the support toolpath planned for a printed part is constructed.

After the toolpath is generated, these paths will be converted by a G-code compiler into the command language to direct the 3D printer fabrication. The G-code compiler here is developed based on Slicer3r and PrusaSlicer [69]. It aims to enable the machine which can adjust the amount of material fed into the machine and the deposition velocity to extrude the required material volume used to print each path to avoid material over extrusion. The amount of material fed into the machine is the product of the cross-section area of a filament (raw material) that multiplies the filament length fed into the machine. The required material volume for printing a toolpath is the result of the cross-section area of this toolpath times its length. A filament's cross-section area is specified by its manufacturer; a toolpath width can be defined by the user; this toolpath thickness is extracted through the slice. By having this information and constricting the deposition velocity as well as identifying this toolpath's length, the length of the filament fed into the machine can be calculated.

b) Selections of slicer settings and the machine

The slicer will process all the test specimens' slices with the same settings; the main process settings are summarised in Table 3. All the test specimens are built with Prusament PLA material and printed using a Prusa MK3 I3 (fused deposition modelling (FDM)) machine; FDM is the most widely used additive manufacturing technology. The specimens for each Test Model are printed in the same position on the build platform and constructed on the same day.

Table 3. Main print settings applied to the slicer

Extrusion Temperature	Build Platform temperature	Infill Angle	Air Gap	Toolpath Width
215 °C	60 °C	45°	0	4.8 mm

c) *Geometric accuracy measurement for physical printed parts*

The physical printed parts' geometric accuracy will be analysed by assessing the profile deviation between each printed part and its digital model. This assessment follows a procedure similar to the geometric accuracy evaluation designed in [70,71] for FDM-constructed parts. This procedure is shown in Figure 6 and can be explained in the following section.

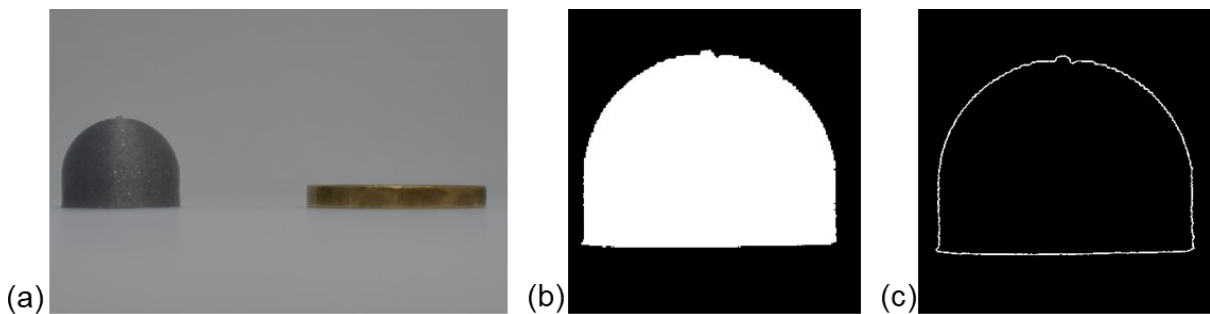


Figure 6. Procedure of detecting printed parts' profile for evaluation. (a) Raw image, (b) convert the truecolor image into a binary image and segment the printed part from this image, (c) edge detection.

Initially, a printed part is placed next to a one-pound coin (with 2.8 mm thickness); the locations of each part and this coin are all fixed in the same position. Each printed part and its coin are photographed using the Nikon digital camera D5200 with a pixel resolution of 6000×4000 . Each image is converted into a binary image using MATLAB Color Thresholder and subsequently processed by MATLAB Image Segmenter to separate the printed part from this binary image. By inputting this segmented image into the MATLAB *bwboundaries* function, the edge profile of a printed part is extracted. This edge profile is then scaled using the ratio of actual coin thickness to the coin thickness (number of pixels) in the image to convert it into its actual size in the printed part. The scaled profiles of all the printed parts of a Test Model will be adjusted by the same scale value to compensate for the thermal shrinkage issue, which generally exists in the printed part and is caused by the thermal stress [72–75]. This value is the average of the ratios of each printed part's scaled

profiles of a Test Model to this model's profile. Next, the adjusted edge profile is aligned with the digital model's profile by overlapping their centroids in order to measure the area of deviation between the two profiles.

Chapter 4: Computational Validations

In this chapter, the accuracy of using volume deviation in assessing the geometric errors in sliced layers is investigated. Further analysis is made to demonstrate the performance of employing this volume deviation measurement in adaptive slicing to optimise the trade-off between build-time reduction and geometric accuracy improvement.

4.1. Performance Tests of Volume Deviation-Based Slicing Methodology

4.1.1. Fixed build time's effect on geometric accuracy

This series of tests looks at the performance of volume deviation-based slicing methodology ($VD_{max}=0.05$) in mitigating the slicing-induced geometric errors, which are sliced layers' volume deviation ratio (VD), staircase effect, and dimensional deviation. Figure 7 shows the maximum, mean, and minimum VD evaluated from each stack of sliced layers generated by these four slicing methodologies. For all Test Models, with the same limitation on the number of sliced layers, volume deviation-based slicing resulted in 2.4–11.1, 1.7–3.5, and 1.1–4.6 times lower sliced layers' maximum VD than those caused by voxelisation-based, cusp height-based, and uniform slicing, respectively. In addition to reducing the maximum VD considerably, the mean VD induced by volume deviation-based slicing was also an average 18.1% lower than the other slicing methodologies. In contrast, half and two-thirds of Test Models, respectively, show that cusp height-based slicing and voxelisation-based slicing caused a larger maximum and mean VD than uniform slicing. Compared to uniform (thinnest) slicing, while it produced an average 48.3% smaller mean VD than volume deviation-based slicing, this reduction was at the cost of largely increasing the number of layers and maximum VD by respectively 1.4–4.8 and 1.2–33.8 times. The minimum VD caused by these slicing did not show a noticeable difference, as most of these Test Models have sections where the only geometric feature is the vertical surface; sliced layers in these sections do not generate geometric deviation.

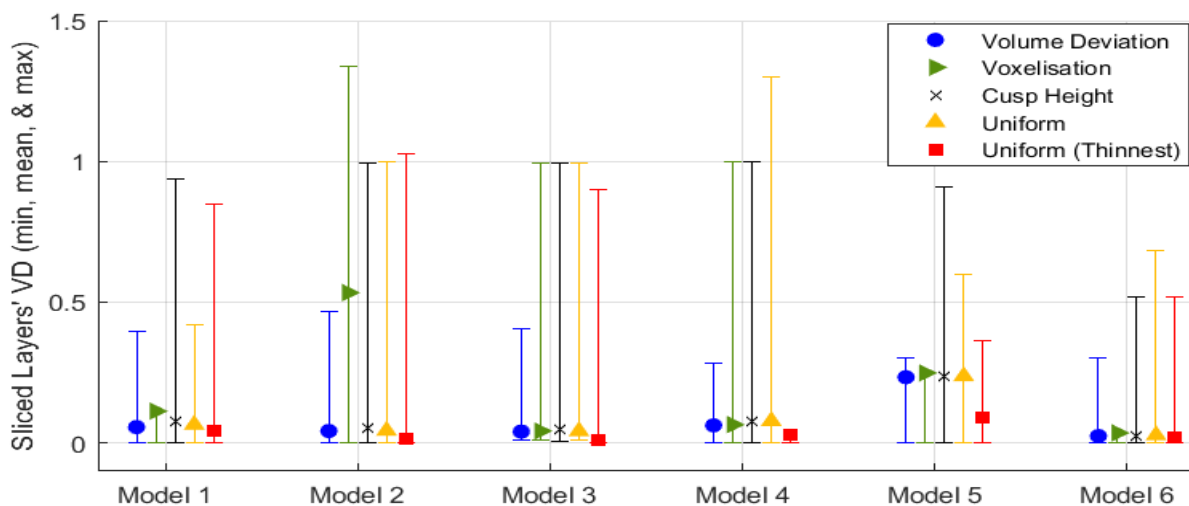


Figure 7. Sliced layers' maximum, mean, and minimum VD induced by slicing Test Models 1–6 using volume deviation-based (blue circle), voxelisation-based (green right-pointing triangle), cusp height-based (back cross) and uniform slicing (upward-pointing yellow triangle for slicing with the same number of layers and red square for slicing with minimum machine-allowable thickness). The sliced layers' maximum VD of uniform (thinnest) slicing on Test Model 3 and voxelisation-based slicing on Test Models 1, 4, and 5, which do not plot on the figure for clarity, are 9.7, 2.6, 2.9, and 3.4, respectively.

Figure 8 aims to present how the sliced layers' VD indicates the presence of the staircase effect and dimensional deviation as well as how these two geometric inaccuracies were affected by the four slicing methodologies. It shows a comparison of the geometry of the (digital) printed part when formed by sliced layers that are generated by these slicing methodologies for Test Model 1. Each printed part reveals the regions with its high volume deviation ratio sections; the red, green, and blue value of each sliced layer's colour within a printed part varies with its volume deviation ratio. For all the printed parts, the regions with a high deviation ratio (greater than 0.1) only existed in the internal cavities, where the staircase effect (in two diamond-shaped cavities) and dimensional deviation (in two rectangular cavities) were observed.

In all the printed parts produced by these slicing, with the same limitation on the number of sliced layers, volume deviation-based slicing resulted in the least prominent staircase effect, particularly in the model's high surface curvature sections (i.e. the two diamond-shaped cavities). It also caused the least dimensional deviation compared to other slicing methodologies, particularly in the flat areas (i.e. the two rectangular cavities). Compared to uniform (thinnest) slicing, volume deviation-based slicing induced a similar degree of the staircase effect to that effect caused by uniform (thinnest) slicing, particularly in the model's high surface curvature sections. However, more dimensional deviations can be seen in the layers generated by uniform (thinnest) slicing than those created by the volume deviation-based technique, especially in the two rectangular cavities.

In contrast to the significant mitigation of the printed parts' geometric inaccuracies achieved by volume deviation-based slicing, the other two adaptive slicing methodologies exhibited more inaccuracies than uniform slicing. The printed part produced by voxelisation-based slicing has the highest level of staircase effect among all the printed parts, particularly in their diamond-shaped cavities. The printed part created by cusp height-based slicing has a slightly lower staircase effect than voxelisation-based slicing in the diamond-shaped cavities. However, it has the largest dimensional deviation in the two rectangular cavities when compared to the printed parts constructed by the other slicing.

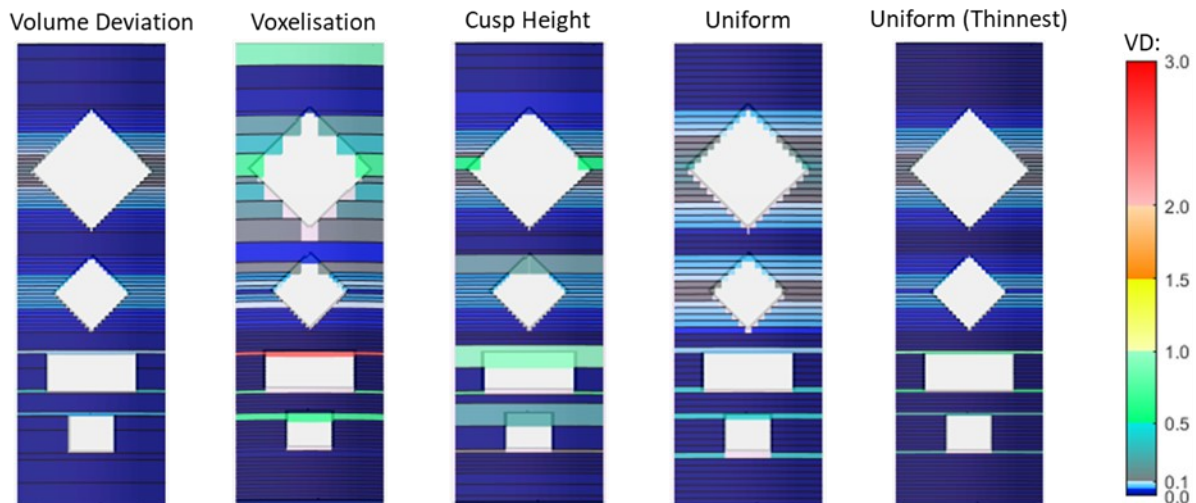


Figure 8. The colourmap of each stack of sliced layers generated by volume deviation-based, voxelisation-based, cusp height-based, and uniform slicing, respectively.

Significant mitigations of the sliced layers' maximum VD, staircase effect, and dimensional deviation (shown in Figures 7 and 8) were accomplished by volume deviation-based slicing compared to other existing slicing methodologies, highlighting its benefits. Volume deviation-based slicing improves the trade-off between build-time reduction and the geometric accuracy improvement compared to the other evaluated slicing methodologies. The achievement of greater geometric accuracy through volume deviation-based slicing is due to its ability to precisely adjust layer thickness according to the variations of surface curvature and geometric complexity. This precise layer thickness adjustment can be demonstrated in Figure 8; volume deviation-based slicing only generated thin-sliced layers in the sections with high surface curvature or near the flat areas to mitigate geometric deviation. The production of thin-sliced layers in these sections demonstrates the greater accuracy of using volume deviation ratio measurement to indicate the surface curvature and geometric complexity variations than the measurement methods applied in voxelisation-based and cusp height-based slicing.

Although volume deviation-based slicing was more limited with regard to mitigating the sliced layers' mean VD than uniform (thinnest) slicing, this does not mean that it produces parts with poorer geometric accuracy than uniform (thinnest) slicing. As shown in Figures 7 and 9, while uniform (thinnest) slicing resulted in a smaller mean VD than volume deviation-based slicing, it produced a greater dimensional deviation; this is because uniform slicing does not consider the model's geometry when slicing. The irrelative relationship between the evaluation of the sliced layers' mean VD and geometric accuracy exists because the mean VD can decrease when increasing the number of sliced layers in a model's low surface curvature or geometric complexity sections. Increasing the number of sliced layers in these

sections will thicken sliced layers in the model's high surface curvature or geometric complexity sections when the number of sliced layers is limited, which will worsen the geometric inaccuracies of the printed parts.

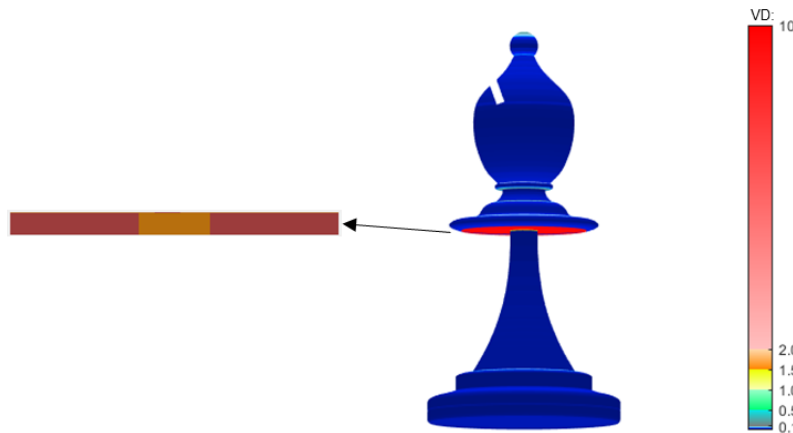


Figure 9. The sliced layer (red) caused a sizeable volume deviation ratio (9.7 VD) from its corresponding region (yellow) in Test Model 4.

Figure 8 also demonstrates that volume deviation-based slicing can achieve a staircase effect in the printed part similar to that of uniform (thinnest) slicing. This similar staircase effect between these two indicates that the staircase effect relating to the part produced by volume deviation-based slicing is not directly induced by the methodology itself, rather it is constrained by the minimum machine-allowable thickness. This constriction suggests that the trade-off between build-time reduction and geometric accuracy improvement can be further optimised by volume deviation-based slicing if the minimum thickness that the machine can manufacture becomes thinner.

In addition to highlighting the benefits of volume deviation-based slicing, the evaluation results of Figures 7 and 8 also reveal the limitations of the other existing adaptive slicing methodologies. The sliced layers' greater maximum VD, staircase effect, and dimensional deviation characterising on the printed parts produced by voxelisation-based and cusp height-based slicing compared to uniform slicing' printed part is due to the inaccurate measurement methods employed in these adaptive slicing. Voxelisation-based slicing simplifies the complex geometric features of the sliced layer and the sliced layer's corresponding region into a set of cubes, resulting inaccurately measuring the geometric deviation between these two. Inaccurately measuring the geometric deviation of sliced layers in the model's low surface curvature and geometric complexity sections can result in a high geometric error, generating thinly sliced layers in these sections. Producing thin-sliced layers increases the number of sliced layers in these sections and limits the layer number in the model's other sections and, thereby causing the inconsistencies between layer thickness variations and model geometric changes. Thus, because of this inconsistent variation and

voxelisation-based slicing generates slices from a model's bottom to its top, this slicing incorrectly produced more slices at the bottom of Test Model 1 than at its top (Figure 8).

Cusp height measurement cannot differentiate the geometric complexity changes and induces an approximate error in indicating surface curvature variations, as explored in the literature review. By lacking the indication of geometric complexity variations, cusp height-based slicing can generate thick-sliced layers in high geometric complexity sections, which induces large dimensional deviations. This incorrect production is the root of causing this slicing to create two thick-sliced layers in the rectangular cavities of Test Model 1. By inaccurately differentiate surface curvature variations, cusp height-based slicing can generate thick-sliced layers in high surface curvature section (e.g. the two thick-sliced layers in diamond-shaped cavities of Test Model 1), resulting in a high staircase effect.

The resulting poor geometric accuracy of the printed parts from voxelisation-based and cusp height-based slicing methodologies compared to uniform slicing conflicts with results from other studies [31,36,43,76]. These studies assessed the printed part's geometric accuracy as achieved by these adaptive slicing methodologies through visual comparison [31,37,44,81] or total mass deviation analysis [43], which caused unreliable investigations, as discussed in section 2.2. These unreliable investigations limited the accuracy of the results of these studies.

4.1.2. Fixed geometric accuracy's effect on build time

This set of experiments aims to investigate the performance of volume deviation-based slicing methodology in reducing the build time by examining the number of sliced layers. This investigation is based on current researchers' consistent identification that increasing the number of layers causes the build time to rise [31,41–43]. Table 4 presents a comparison of the number of sliced layers that resulted from volume deviation-based, voxelisation-based, cusp height-based, and uniform slicing under the limitation of a similar geometric accuracy degree; Figure 10 shows the geometric accuracy induced by these methodologies. To limit the geometric accuracy of volume deviation-based slicing, the author defined its VD_{max} by using the third quartile of the voxelisation's box. For Test Model 1, volume deviation-based slicing respectively produced 38%, 42%, and 44% fewer layers than voxelisation-based, cusp height-based, and uniform slicing. For Test Model 4, the reduction in the number of sliced layers by volume deviation-based slicing was less significant than that found in Test Model 1. However, the considerable mitigation of the number of sliced layers accomplished by volume deviation-based slicing compared to the other three slicing methodologies can still be observed clearly. It decreased the number of sliced layers by 12%, 24%, and 32%

compared to voxelisation-based, cusp height-based slicing, and uniform slicing, respectively. Despite volume deviation-based slicing reducing the number of sliced layers considerably, it still significantly decreased the sliced layer's large VD (i.e. the outliers) compared to the other three slicing methodologies (Figure 10).

Table 4. The number of sliced layers generated by slicing methodologies when the printed part's geometric accuracy is limited by the need for a similar geometric accuracy degree.

Specimens	Volume Deviation	Voxelisation	Cusp Height	Uniform
Test Model 1	56	90	97	100
Test Model 4	176	200	231	260

* The unit of measurement for all of the data is the number of sliced layers.

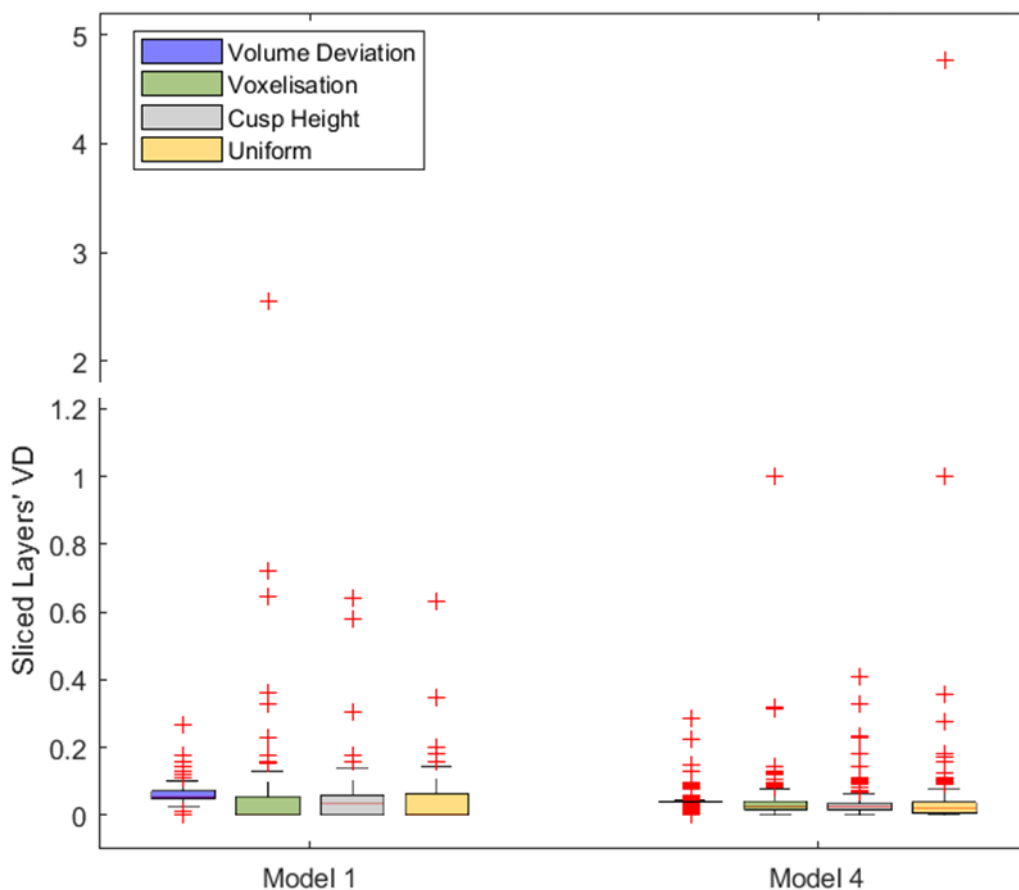


Figure 10. Sliced layers' VD induced by slicing Test Models 1 and 4 using volume deviation-based (blue), voxelisation-based (green), cusp height-based (grey) and uniform slicing (yellow); the number of sliced layer for each stack of sliced layers generated by these slicing methodologies is summarised in Table 4

The considerable mitigation of the number of sliced layers accomplished by volume deviation-based slicing was because this slicing has better accuracy in adjusting each layer thickness according to the model's geometry than other existing slicing methodologies, as

evaluated in section 4.1.1. This precise thickness modification enables producing thick-sliced layers in low surface curvature and geometric complexity sections to reduce build time and generating thin-sliced layers in other sections to improve geometric accuracy. The enhanced geometric accuracy explains why volume deviation-based slicing resulted in smaller sliced layer's VD (outliers) than the other slicing methodologies. The mitigation of the sliced layer's VD and the number of sliced layers demonstrates that volume deviation-based slicing has a better performance in reducing build time while optimising geometric accuracy than the other evaluated slicing methodologies.

The build-time reduction accomplished by volume deviation-based slicing was observed to have varied slightly from model to model. The degree of reducing the number of sliced layers achieved by volume deviation-based slicing investigated from Test Model 1 was approximately two times more than its reduction of the number of sliced layers in Test Model 4. The more degree of sliced-layer reduction was investigated from Test Model 1 because it contains larger areas with low curvature and geometric complexity than Test Model 4. These large areas of Test Model 1 enabled volume deviation-based slicing to have more sections to generate thick-sliced layers than Test Model 4. In contrast, the larger areas of Test Model 1 (than Test Model 4) also provided more sections for voxelisation-based, cusp height-based, and uniform slicing to mistakenly produce thin-sliced layers, as evaluated in section 4.1.1. The thick and thin layers respectively generated by volume deviation-based slicing and other slicing methodologies in these sections enlarged the difference between the respective number of sliced layers that they each produced.

4.2. Evaluating the Fairness of Comparison

This test focused on evaluating the fairness of the above comparison between voxelisation-based and volume deviation-based slicing. This comparison was conducted because the voxel size of voxelisation-based slicing in the above comparison was larger than that used in its original paper, as discussed in the experimental methods section. To increase the number of voxels used to represent each sliced layer and its corresponding region, the author enlarged the size of the digital models and the machine-allowable thicknesses by 1,500%. This is because the maximum-allowable thickness and the maximum height of digital models that can be processed in the IceSL slicer are, respectively, 5 mm and approximately 500 mm. Figure 11 presents the comparison of the geometry of the part formed by the same number of sliced layers that were generated by voxelisation-based slicing before and after voxelisation resolution improvement.

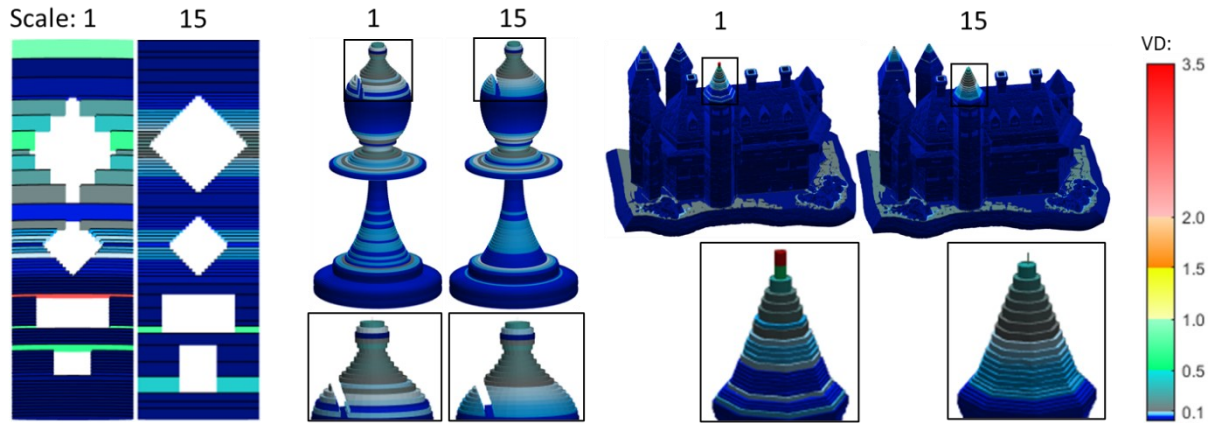


Figure 11. Colourmap of each stack of sliced layers generated by voxelisation-based slicing before and after voxelisation resolution improvement. Scale: 1 indicates slicing using the original models' size and machine-allowable thickness, while 15 refers to slicing by enlarging the models' size and allowable thickness by 1,500%. The zoom-in areas in each stack of sliced layers are the critical regions (small volume sections with a high surface curvature and geometric complexity) of the Test Models. The slices of Test Models 4 and 6 are not shown on the figure for clarity.

After increased voxelisation resolution by 15 times in voxelisation-based slicing, the printed part's staircase effect mitigation can only be observed clearly in Test Model 6's two diamond-shaped cavities compared to those parts created with its original resolution. In addition to the staircase effect mitigation limited by the model's geometry, an increased dimensional deviation was also revealed in the two rectangular cavities of this model. In Test Models 4 and 6, increasing the voxelisation resolution of voxelisation-based slicing reduced only the volume deviation ratio in these model's large sections slightly but raised this ratio and the staircase effect in the small sections. These small sections are the critical regions shown in Figure 11. Compared to volume deviation-based slicing (Figure 12), voxelisation-based slicing with an increased voxelisation resolution still resulted in a more significant dimensional deviation in Test Model 1 and a higher staircase effect in Test Models 4 and 6.

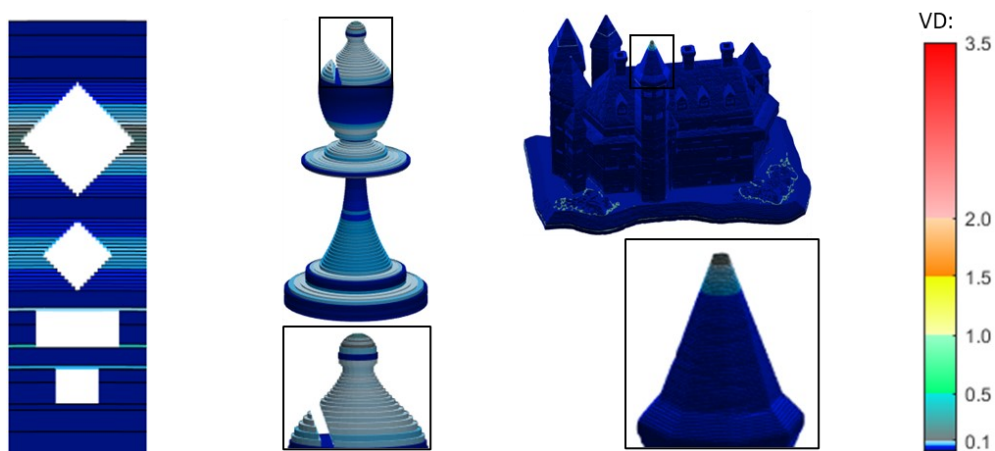


Figure 12. Colourmap of each stack of sliced layers generated by volume deviation-based slicing; these sliced layers were generated with the original models' size (scale 1) and machine-allowable thickness.

Figures 11 and 12 demonstrate that increasing the voxelisation resolution in voxelisation-based slicing is limited with regard to improving the geometric accuracy of the printed parts. Voxelisation approximately represents a model's geometry by a set of cubes. Increasing the voxelisation resolution mitigates this approximation; this mitigated approximation reduces the measurement error when evaluating the sliced layer's geometric deviation. This reduced measurement error explains why the staircase effect in the two diamond-shaped cavities of Test Model 1 was reduced. However, an increased dimensional deviation in Test Model 1 and aggravated geometric inaccuracies (volume deviation ratio and staircase effect) in Test Models 4 and 6 were also observed.

The increased dimensional deviation caused by improving the voxelisation resolution is similar to the issue discussed for uniform slicing with minimum machine-allowable thickness in literature review. The heights of each voxelised sliced layer and its voxelised corresponding region are defined by accumulating the voxels' height. Thus, when a dimensional specification (height) cannot be exactly divided by the voxel's height, a measurement error in evaluating each sliced layer's geometric deviation occurs.

In addition to increasing dimensional deviation, the geometric inaccuracy aggravation resulting from an increased voxelisation resolution is due to the voxelisation-based slicing modifying each layer thickness based directly on the volume of the sliced layer's geometric deviation. Directly assessing this volume does not take into consideration how well the sliced layer represents its corresponding region's geometric features. As the model's small volume sections result in a small geometric error (volume), thick-sliced layers can then be generated by voxelisation-based slicing in small volume sections with high surface curvature or geometric complexity. This small geometric error may be further decreased by reducing the measurement approximation through improving voxelisation resolution. This reduction of geometric error can further thicken the sliced layers in models' small sections with high surface curvature or geometric complexity, aggravating the geometric inaccuracies in these sections. These aggravated geometric inaccuracies and the occasional staircase effect mitigation indicate the limited relationship between printed parts' geometric inaccuracies and the voxelisation resolution of voxelisation-based slicing. This limited relationship demonstrates that the above comparison between voxelisation-based slicing (with a relatively lower resolution than in the original paper) and volume deviation-based slicing was fair.

4.3. Conclusions on Computational Validations

Volume deviation-based slicing has been evaluated computationally here; analysis have shown that it outperforms existing slicing methodologies in optimising the trade-off between build-time reduction and geometric accuracy improvement. Results were found from analysing the geometric accuracy changes by limiting the build time (number of sliced layers) and from investigating the build time differences through constraining the geometric accuracy.

Volume deviation-based slicing caused the least volume deviation ratio, staircase effect, and dimensional deviation in the printed part compared to existing slicing methodologies within the limitation requiring the same number of sliced layers. It can also reduce the build time by nearly half in comparison with current slicing methodologies under the limitation of a similar degree of their printed parts' geometric accuracy. These two achievements evaluated under different user-defined tolerances show the repeatability of this slicing' performance. This repeatability is attributed to the precise adjustment of layer thicknesses according to the model's geometry (the variations of surface curvature and geometric complexity).

The analysis from fixed geometric accuracy's effect on build time also shown that the degree of build time reduced by volume deviation-based slicing is also affected by the model's geometry. This result suggests a guide of using volume deviation-based slicing. That is, it will work similarly to uniform slicing when the model's geometry is not changed along its Z-axis (e.g. cube, vertical cylinder, and regular tetrahedron); this type of model does not have suitable areas for allowing variations in layer thickness.

Chapter 5: Manufacturing Validations

This chapter presents and discusses the results of validating volume deviation-based, voxelisation-based, and uniform slicing using physical printed parts. These parts were constructed using the sliced layers used to assess these slicing methodologies in the previous chapter. Validations were made by analysing the area discrepancy between the profile of the printed part and the profile of this printed part's digital model.

5.1. Manufacturing Results and Discussions

The validations in this chapter follow the manufacturing experiments designed in Chapter 3 and aim to investigate whether the demonstrated result gained from digital printed parts can also be observed in physical fabricated parts. Figures 13 and 14 show the comparisons between the triangulated surface profiles of Test Models (2 and 4) and the profiles of their corresponding printed parts, which were manufactured using volume deviation-based, voxelisation-based, and uniform slicing. The area discrepancy between the contour of each (fabricated) layer in a constructed part and the layer's corresponding region in the digital model's contour is presented along with the profile comparison of the printed part.

Figure 13 shows the results of these two evaluations for the three slicing methodologies on Test Model 2. Volume deviation-based and voxelisation-based slicing resulted in less area discrepancy than uniform slicing, particularly the fabricated layers in the top sections of the printed part. The area discrepancy of each layer built with uniform slicing continually increased from the middle to the last layer, as the curvature of these layers' corresponding regions constantly increased. These area discrepancies caused a staircase effect that can be clearly observed around the top sections of the profile of the part made by this slicing. However, there is not a significant difference between the geometry and area discrepancy of the parts printed by volume-deviation based slicing and voxelisation-based slicing. A positive discrepancy with a fluctuating shape, and a negative discrepancy with a flat shape, can be respectively observed from the top of the profile of parts printed by volume deviation-based slicing and voxelisation-based slicing.

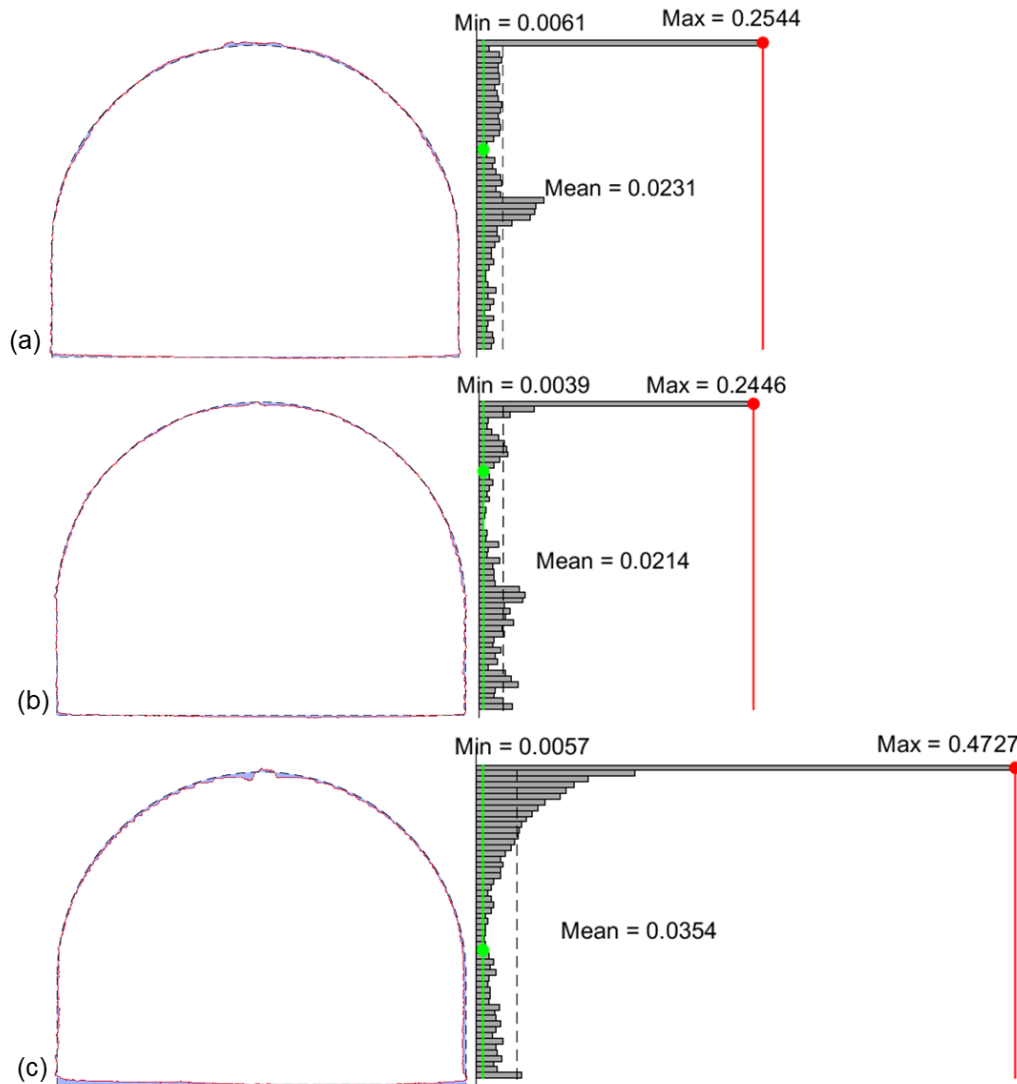


Figure 13. The deviation (blue area) between the 2D designed shape (dashed line) of Test Model 2 and the profile (solid line) of the parts, which were printed by using volume-deviation based (a), voxelisation-based (b), and uniform slicing (c). The bar graph next (right) to each profile analysis presents the area of the discrepancy between each fabricated layer contour and its corresponding region shape; the Y-axis of each bar element indicates the layer number (from 2nd to 56th), while the X-axis represents the discrepancy area (cm²). For results clarity, the discrepancy in the first layer is not shown. This layer has a risk of wrapping due to thermal stress caused by uneven heat distribution and has a high risk of a slight shape distortion incurred by the operator when removing the printed part from the build platform. These risks may affect the analysis accuracy of evaluating the geometric inaccuracies of printed parts induced by only the slicing.

Figure 14 shows the assessment results of the fabricated parts of Test Model 4. From the profile comparisons, volume deviation-based slicing resulted in bringing the printed part's profile closer to its designed shape than the other two slicing methodologies, particularly the high surface curvature (bishop's top) and geometric complexity (flat overhang) sections. In addition to bringing the print profile closer to its designed shape, volume deviation-based slicing also caused the least maximum area discrepancy among all the fabricated layers in its constructed part compared to the other two slicing methodologies. Volume deviation-based slicing significantly reduced the maximum area discrepancy by 63.74% and 72.60%,

respectively, from the parts manufactured by voxelisation-based and uniform slicing. However, voxelisation-based slicing induced only 12.12% less maximum area discrepancy than uniform slicing. This limited mitigation of geometric inaccuracies can also be observed in comparing the profiles of the printed parts made by voxelisation-based and uniform slicing. Although the constructed part created by voxelisation-based slicing is slightly closer to its designed shape in its flat overhanging section than that fabricated by uniform slicing, it deviates further from the designed shape in its top sections compared to uniform slicing.

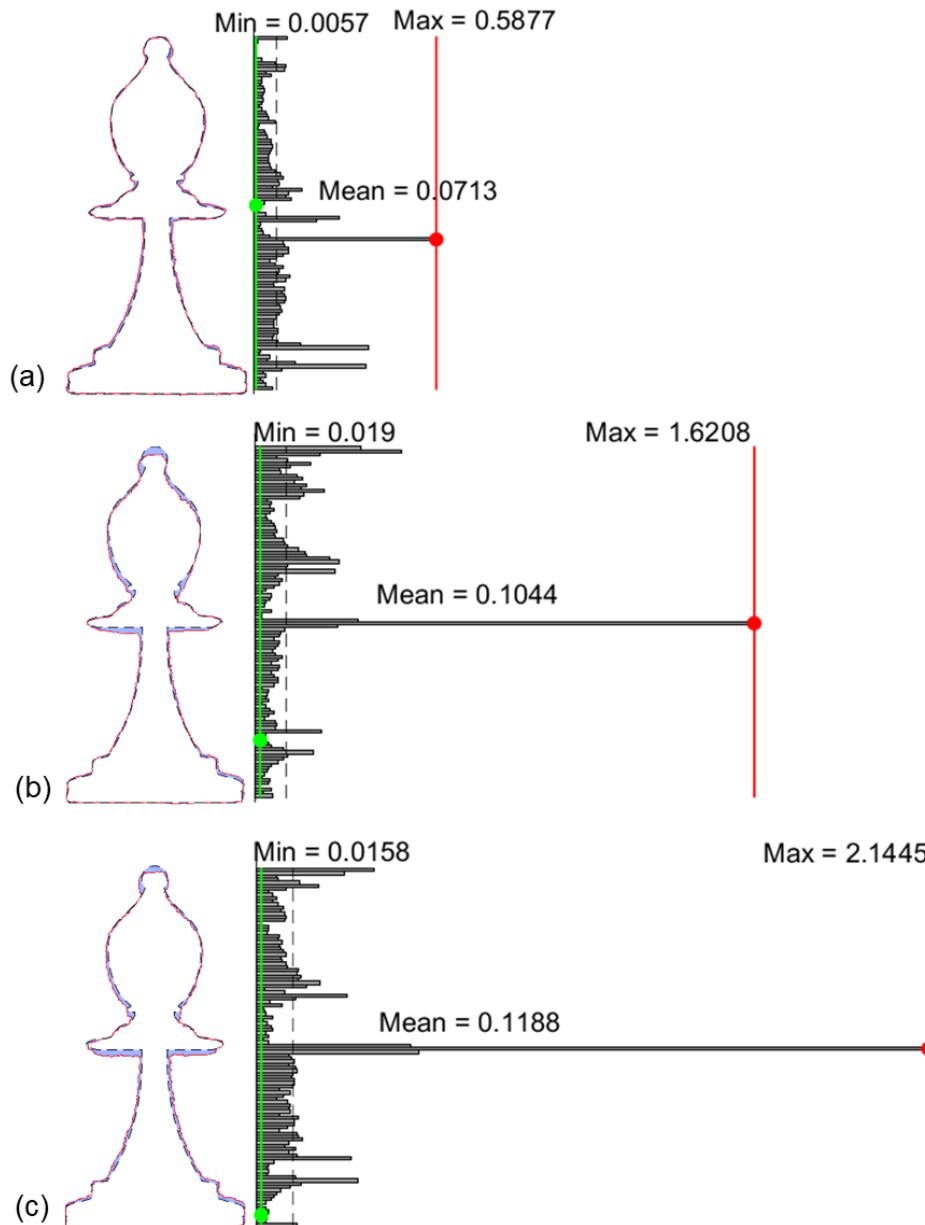


Figure 14. The deviation (blue area) between the 2D designed shape (dashed line) of Test Model 4 and the profile (solid line) of the parts, which were printed by using volume-deviation based (a), voxelisation-based (b), and uniform slicing (c). The bar chart next (right) to each profile analysis shows the area of the discrepancy between each fabricated layer contour and its corresponding region shape; the Y-axis of each bar element indicates the layer number (2nd to 115th), while the X-axis represents the discrepancy area (cm²). For results clarity, the discrepancy in the first layer is not shown.

Figures 13 and 14 demonstrate the transfer of the better geometric accuracy accomplished by volume deviation-based slicing than voxelisation-based and uniform slicing (within the limitation requiring the same number of sliced layers) from computation to physical fabricated parts. Consistent with the results from computational validations, volume deviation-based slicing mitigated the deviation between the print profile and the designed shape considerably compared to the other two slicing methodologies, particularly on Test Model 4. This mitigation resulted because volume deviation-based slicing precisely assesses the sliced layer's geometric deviation and modifies its thickness until its volume deviation ratio is within a user-specified tolerance. By accurately measuring the sliced layer's geometric deviation, volume deviation-based slicing varies each layer thickness consistently with the variations of the model geometry, as analysed in Chapter 4. By limiting each layer's volume deviation ratio, the geometric deviation induced by each layer is restricted. This restricted geometric deviation caused volume deviation-based slicing to produce fabricated layers with the smallest area discrepancy (minimum, mean, and maximum) compared to the other two slicing methodologies, as evident in Figure 14.

A similar geometric accuracy (profile deviation and area discrepancy) was observed from the printed parts made by volume deviation-based and voxelisation-based slicing in printing Test Model 2. Volume deviation-based and voxelisation-based slicing respectively produced a positive and a negative discrepancy in the top of printed parts (Figure 14). However, this result does not indicate that these two slicing methodologies optimised the same degree of geometric accuracy in these printed parts. The positive discrepancy was not induced by slicing because the sliced layers (from the 49th to the last) in the top sections were generated by volume deviation-based slicing with the minimum machine allowable thickness, as shown in Figure 15 (a). This positive discrepancy was induced by a slight over extrusion (Figure 15 (b)) in printing the last layers, which may be due to the slow nozzle travel speed and high extrusion temperature while printing the fine details [77,78]. This over-extrusion issue caused molten material to accumulate between the nozzle and the fabricated layer while the nozzle was travelling slowly; this accumulated material resulted in stringing (Figure 15 (c)) when the nozzle was lifted from the printed part. These material strings are the roots of causing the shape of this positive discrepancy to fluctuate. In contrast, a negative discrepancy resulted from the staircase effect induced by thick-sliced layers created by voxelisation-based slicing in the model's high curvature sections. The generation of these thick-sliced layers in the top sections can be observed in Figure 15 (a) and is due to the inconsistency between layer thickness adjustment and surface curvature variations in voxelisation-based slicing, as evaluated in computational validations. The negative discrepancy induced by the inaccurate layer thickness modification of voxelisation-based

slicing further highlights the benefit of volume deviation based-slicing in optimising the trade-off between build-time reduction and geometric accuracy improvement. The positive discrepancy resulting from print issues suggests that a better control of print parameter settings (that mitigate these issues) is needed when implementing volume deviation-based slicing on the machine, thereby releasing the full benefit of this slicing.

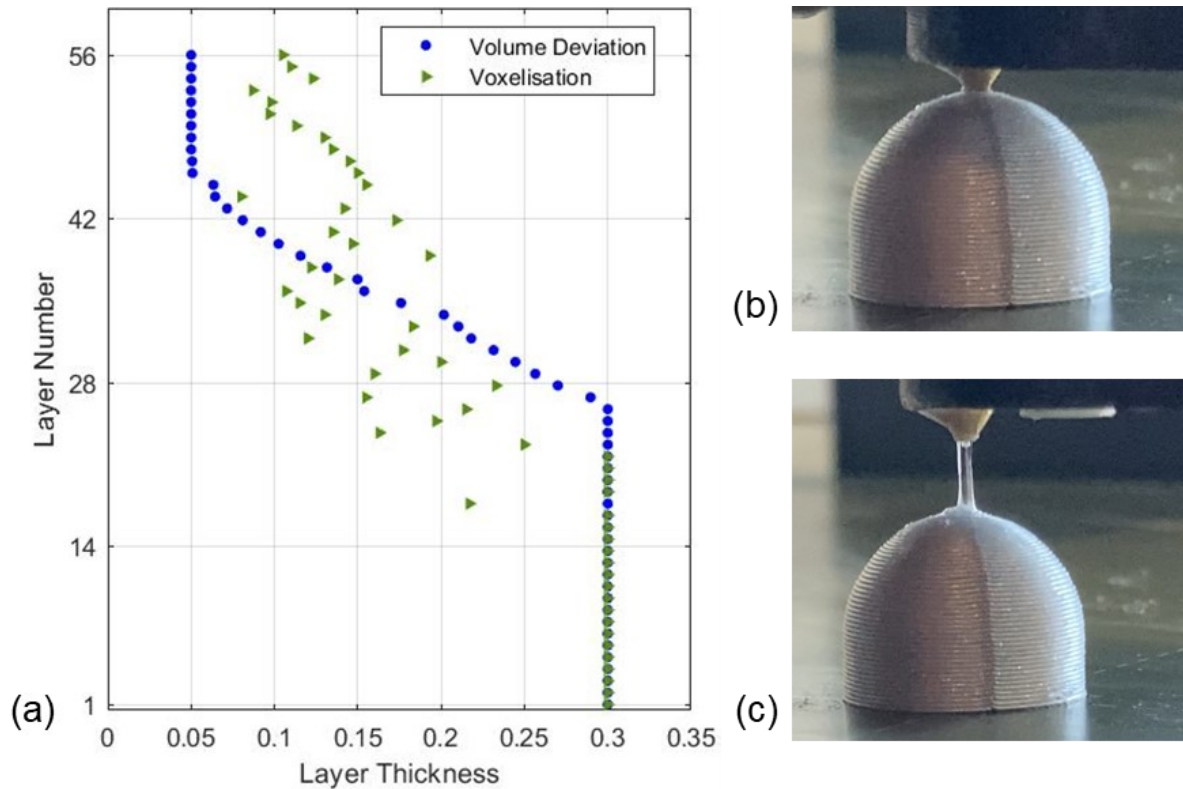


Figure 15. (a) The thickness of each sliced layer produced by volume deviation-based (blue circle) and voxelisation-based slicing (green right-pointing triangle) for Test Model 2 against the layer number. The shape of the last layer of the part printed by using volume deviation-based slicing during (b) and after (c) fabricating this layer.

5.2. Conclusions on Manufacturing Validations

This investigation has shown the benefits of volume deviation-based slicing on physical fabricated parts. Volume deviation-based slicing optimised the trade-off between build-time reduction and geometric accuracy improvement better than other existing slicing methodologies, as consistent with the results from computational validations. This identification was found by assessing the deviation between the print profile and the designed shape. Test Models 2 and 4 and the slicing methodologies of volume deviation-based, voxelisation-based, and uniform slicing were employed in this assessment.

The evaluations from Test Model 4 show volume deviation-based slicing produced the print profile closer to the designed shape than both voxelisation-based and uniform slicing. This

result is attributed to the strong consistency between the layer thickness modifications and the model geometric variations in volume deviation-based slicing.

Through investigating the test specimens of Test Model 2, the parts printed by volume deviation-based slicing and voxelisation-based slicing were showed a similar degree of geometric accuracy. This result, which conflicts with that from computational validations, was incurred by the print issue (over extrusion) in implementing volume deviation-based slicing. This print issue suggests that controlling the print parameters to direct the machine to fabricate the part following exactly the toolpath planned by the slicer is essential to reap the benefits of volume deviation-based slicing. This direction of the machine fabrication could be accomplished by employing the methodologies of print processes monitoring and closed-loop control [79]. For example, the image analysis-based closed-loop quality control methodology developed by Liu et al. [80] can be used to adjust the extrusion speed and temperature during fabrication to avoid the over-extrusion issue.

Chapter 6: Conclusions and Suggestions for Future Works

Volume deviation-based slicing has been proposed. This slicing has been validated using computation and manufacturing. This chapter summarises the findings of this study and provides suggestions for future research.

This project has proposed a novel adaptive slicing methodology that adjusts each layer thickness based on the ratio of the volume of each sliced layer's geometric error to the volume of its corresponding region in the digital model for layer-based additive manufacturing. To the best of the author's knowledge, this is the first approach to modify each layer thickness without approximately measuring the sliced layer's geometric deviation. By accurately assessing each sliced layer's geometric error, this slicing can correctly identify both the variations of surface curvature and geometric complexity of the model and, therefore, precisely adjust each layer thickness by following these variations. This precise layer modification enables volume deviation-based slicing to outperform existing slicing methodologies in optimising the trade-off between build-time reduction and geometric accuracy improvement. This finding was demonstrated in both the computational and manufacturing validations.

Computational validations showed that volume deviation-based slicing caused the least volume deviation ratio, staircase effect, and dimensional deviation in (digital) printed parts compared to voxelisation-based, cusp height-based, and uniform slicing within the limitation of the same number of sliced layers. Within the limitation of a similar geometric accuracy degree, volume deviation-based slicing can reduce build time by nearly half compared to the other slicing methodologies. Investigations found that the degree of build-time reduction accomplished by this slicing can be affected by the model's geometry. This finding suggests volume deviation-based slicing should not be recommended when the model's geometry is not changed along its Z-axis (e.g. cube, vertical cylinder, and regular tetrahedron) compared to uniform slicing, which does not require computing the geometric error repetitively. Although the computational time may be increased when using volume deviation-based slicing compared to uniform slicing, this computation-time penalty can be compensated (or even ignored) by reducing the total manufacturing time, particularly when large quantities are being produced. This lessening of the total manufacturing duration is the result of volume deviation-based slicing reducing fabrication time and potentially decreasing the amount of post-processing time required by improving the printed part's geometric accuracy.

Manufacturing validations demonstrated that volume deviation-based slicing can bring the profile of the printed part closer to its designed shape than the voxelisation-based and uniform slicing. However, the degree of geometric inaccuracies of the physical fabricated part printed by volume deviation-based slicing was occasionally shown to be similar to that of the part printed by voxelisation-based slicing (i.e. in Test model 2). This result was caused by the print issue of over extrusion, according to the analyses of the layer thicknesses adjusted by these two slicing methodologies and the fabrication processes investigations. It

is thus suggested that controlling the print parameters to avoid print issues is vital to utilising the advantages of volume deviation-based slicing. While manufacturing validations were conducted using the FDM machine, volume deviation-based slicing can also be applied to most of the other current AM machines, as they share a common digital thread. For example, stereolithography, powder bed fusion, and direct energy deposition.

This research did not directly present the effect of the changes of user-defined tolerance on slicing performance. That is because its results are straightforward; the greater the tolerance, the poorer geometric accuracy due to each sliced layer being generated to be allowed to contain more errors, the less build time.

Future research could be conducted to investigate the print parameter controls during AM machine fabrication. While much work has been done to develop closed-loop control systems for AM machines, most of these systems were designed for extrusion-based techniques [81]. By developing systems that eliminate the print issues and by employing volume deviation-based slicing to mitigate the slicing-induced geometric inaccuracies, ultimately, there is a possibility of eliminating the geometric inaccuracies of printed parts.

In addition to developing control systems, future work could also be done to incorporate volume deviation-based slicing to non-planar layer slicing to simultaneously mitigate the geometric inaccuracies and mechanical anisotropy of AM-fabricated parts. Integrating these two slicing methodologies is desirable because most current non-planar layer slicing methodologies were developed with the sole focus on mechanical anisotropy mitigation, as discussed in Chapter 2. This incorporation could be achieved by using the non-planar layer slicing to produce curved-sliced layers for mechanical anisotropy mitigation while using the volume deviation based-slicing to adjust each layer thickness for geometric accuracy improvement.

References

1. Minshall T, Featherston C. A Case Study of the development of the UK's Additive Manufacturing National Strategy 2014-2017. 2019;
2. Urhal P, Weightman A, Diver C, Bartolo P. Robot assisted additive manufacturing: A review. *Robotics and Computer-Integrated Manufacturing*. 2019 Oct 1;59:335–45.
3. Steuben JC, Iliopoulos AP, Michopoulos JG. Implicit slicing for functionally tailored additive manufacturing. *CAD Computer Aided Design*. 2016 Aug 1;77:107–19.
4. Danjou S, Köhler P. Improving part quality and process efficiency in layered manufacturing by adaptive slicing. *Virtual and Physical Prototyping*. 2010 Dec 8;5(4):183–8.
5. Daneshmand S, Aghanajafi C, Ahmadi Nadooshan A. The effect of chromium coating in RP technology for airfoil manufacturing. *Sadhana - Academy Proceedings in Engineering Sciences* [Internet]. 2010 Oct [cited 2021 Aug 11];35(5):569–84. Available from: <https://www.semanticscholar.org/paper/The-effect-of-chromium-coating-in-RP-technology-for-Daneshmand-Aghanajafi/daad7e70369377e602fb860ce8e15fd9497bca9c>
6. Junk S, Schröder W, Schrock S. Design of Additively Manufactured Wind Tunnel Models for Use with UAVs. *Procedia CIRP*. 2017 Jan 1;60:241–6.
7. Zhu W. Models for wind tunnel tests based on additive manufacturing technology. *Progress in Aerospace Sciences*. 2019 Oct 1;110:100541.
8. Magerramova L, Vasilyev B, Kinzburskiy V. Novel Designs of Turbine Blades for Additive Manufacturing. *Proceedings of the ASME Turbo Expo* [Internet]. 2016 Sep 20 [cited 2021 Aug 11];5C-2016. Available from: <http://asmedigitalcollection.asme.org/GT/proceedings-pdf/GT2016/49804/V05CT18A001/2431061/v05ct18a001-gt2016-56084.pdf>

9. Lee P-H, Chung H, Lee SW, Yoo J, Ko J. Review: Dimensional Accuracy in Additive Manufacturing Processes. ASME 2014 International Manufacturing Science and Engineering Conference, MSEC 2014 Collocated with the JSME 2014 International Conference on Materials and Processing and the 42nd North American Manufacturing Research Conference [Internet]. 2014 Oct 3 [cited 2021 Aug 11];1. Available from: <http://asmedigitalcollection.asme.org/MSEC/proceedings-pdf/MSEC2014/45806/V001T04A045/4425314/v001t04a045-msec2014-4037.pdf>
10. Tiwary VK, Arunkumar P, Deshpande AS, Rangaswamy N. Surface enhancement of FDM patterns to be used in rapid investment casting for making medical implants. *Rapid Prototyping Journal*. 2019 Aug 21;25(5):904–14.
11. Chohan JS, Singh R. Pre and post processing techniques to improve surface characteristics of FDM parts: a state of art review and future applications. *Rapid Prototyping Journal*. 2017;23(3):495–513.
12. Singh D, Singh R, Boparai KS. Development and surface improvement of FDM pattern based investment casting of biomedical implants: A state of art review. *Journal of Manufacturing Processes*. 2018 Jan 1;31:80–95.
13. Singh J, Singh R, Singh H. Dimensional accuracy and surface finish of biomedical implant fabricated as rapid investment casting for small to medium quantity production. *Journal of Manufacturing Processes*. 2017 Jan 1;25:201–11.
14. Lee JY, Nagalingam AP, Yeo SH. A review on the state-of-the-art of surface finishing processes and related ISO/ASTM standards for metal additive manufactured components. *Virtual and Physical Prototyping* [Internet]. 2021 [cited 2021 Jun 3];16(1):68–96. Available from: <https://www.tandfonline.com/action/journalInformation?journalCode=nvpp20>
15. Prospera Sibanda SIBANDA, Peter CARR, Michael RYANA, Samuel BIGOT. State of The Art in Surface Finish of Metal Additive Manufactured Parts. In: Conference: ICMR [Internet]. Belfast; 2019 [cited 2021 Jun 2]. Available from: https://www.researchgate.net/publication/345309117_State_of_The_Art_in_Surface_Finish_of_Metal_Additive_Manufactured_Parts
16. Morton W, Green S, Rennie AEW, Abram TN. Surface finishing techniques for SLM manufactured stainless steel 316L components [Internet]. Paulo Jorge da Silva Bartolo, editor. *Innovative Developments in Virtual and Physical Prototyping*. Leiria:

- CRC Press; 2012 [cited 2021 Jun 2]. 503–509. Available from: https://www.researchgate.net/publication/300064369_Surface_finishing_techniques_for_SLM_manufactured_stainless_steel_316L_components
17. Hashmi AW, Mali HS, Meena A. The Surface Quality Improvement Methods for FDM Printed Parts: A Review. In: Harshit K. DaveJ, Paulo Davim, editors. Fused Deposition Modeling Based 3D Printing [Internet]. 1st ed. Springer, Cham; 2021 [cited 2021 Jun 2]. p. 167–94. Available from: https://doi.org/10.1007/978-3-030-68024-4_9
 18. Boschetto A, Bottini L. Surface improvement of fused deposition modeling parts by barrel finishing. Rapid Prototyping Journal [Internet]. 2015 Oct 19 [cited 2021 Jun 3];21(6):686–96. Available from: <https://www.emerald.com/insight/content/doi/10.1108/RPJ-10-2013-0105/full/html>
 19. Kim H, Lin Y, Tseng TLB. A review on quality control in additive manufacturing [Internet]. Vol. 24, Rapid Prototyping Journal. Emerald Group Publishing Ltd.; 2018 [cited 2021 Jun 3]. p. 645–69. Available from: <https://www.emerald.com/insight/content/doi/10.1108/RPJ-03-2017-0048/full/html?fullSc=1>
 20. Chohan JS, Singh • Rupinder, Kamaljit •, Boparai S. Post-processing of ABS Replicas with Vapour Smoothing for Investment Casting Applications. Proceedings of the National Academy of Sciences, India Section A: Physical Sciences [Internet]. 2019 [cited 2021 Jun 3]; Available from: <https://doi.org/10.1007/s40010-020-00669-x>
 21. Jayanth N, Senthil P, Prakash C. Effect of chemical treatment on tensile strength and surface roughness of 3D-printed ABS using the FDM process. Virtual and Physical Prototyping [Internet]. 2018 Jul 3 [cited 2021 Jun 8];13(3):155–63. Available from: <https://www.tandfonline.com/action/journalInformation?journalCode=nvpp20>
 22. Busachi A, Erkoyuncu J, Colegrove P, Martina F, Watts C, Drake R. A review of Additive Manufacturing technology and Cost Estimation techniques for the defence sector. CIRP Journal of Manufacturing Science and Technology. 2017 Nov 1;19:117–28.
 23. Baumers M, Beltrametti L, Gasparre A, Hague R. Informing additive manufacturing technology adoption: total cost and the impact of capacity utilisation. International Journal of Production Research. 2017 Dec 2;55(23):6957–70.

24. Achilles C, Tzetzis D, Raimondo MO. Alternative production strategies based on the comparison of additive and traditional manufacturing technologies. *International Journal of Production Research*. 2017;55:3497–509.
25. Lanzotti A, Martorelli M, Staiano G. Understanding process parameter effects of rewrap open-source three-dimensional printers through a design of experiments approach. *Journal of Manufacturing Science and Engineering, Transactions of the ASME*. 2015 Feb 1;137(1).
26. Paul BK, Voorakarnam V. Effect of layer thickness and orientation angle on surface roughness in laminated object manufacturing. *Journal of Manufacturing Processes*. 2001 Jan 1;3(2):94–101.
27. García Plaza E, Núñez López PJ, Caminero Torija MÁ, Chacón Muñoz JM. Analysis of PLA geometric properties processed by FFF additive manufacturing: Effects of process parameters and plate-extruder precision motion. *Polymers*. 2019 Jan 1;11(10):1581.
28. Nath P, Olson JD, Mahadevan S, Lee YTT. Optimization of fused filament fabrication process parameters under uncertainty to maximize part geometry accuracy. *Additive Manufacturing*. 2020 Oct 1;35:101331.
29. Chen H, Zhao YF. Process parameters optimization for improving surface quality and manufacturing accuracy of binder jetting additive manufacturing process. *Rapid Prototyping Journal*. 2016;22(3):527–38.
30. Geng Z, Bidanda B. Geometric precision analysis for Additive Manufacturing processes: A comparative study. *Precision Engineering*. 2021 May 1;69:68–76.
31. Mao H, Kwok TH, Chen Y, Wang CCL. Adaptive slicing based on efficient profile analysis. *CAD Computer Aided Design* [Internet]. 2019 Feb 1 [cited 2020 Jun 16];107:89–101. Available from: <https://www.sciencedirect.com/science/article/pii/S0010448518301763>
32. Fu G, Fu J, Lin Z, Shen H, Jin Y. A polygons Boolean operations-based adaptive slicing with sliced data for additive manufacturing. *Proceedings of the Institution of Mechanical Engineers, Part C: Journal of Mechanical Engineering Science*. 2017 Aug 24;231(15):2783–99.

33. Singhal SK, Jain PK, Pandey PM. Adaptive Slicing for SLS Prototyping. *Computer-Aided Design & Applications*. 2008;5(4):412–23.
34. Huang B, Singamneni SB. Curved layer adaptive slicing (CLAS) for fused deposition modelling. *Rapid Prototyping Journal*. 2015 Jun 15;21(4):354–67.
35. Mani K, Kulkarni P, Dutta D. Region-based adaptive slicing. *CAD Computer Aided Design*. 1999 Apr 30;31(5):317–33.
36. Danjou S, Köhler P. Improving part quality and process efficiency in layered manufacturing by adaptive slicing. *Virtual and Physical Prototyping*. 2010 Dec 8;5(4):183–8.
37. Yang Y, Fuh JYH, Loh HT, Wong YS. A volumetric difference-based adaptive slicing and deposition method for layered manufacturing. *Journal of Manufacturing Science and Engineering, Transactions of the ASME*. 2003 Aug 1;125(3):586–94.
38. Zhao Z, Laperrière L. Adaptive direct slicing of the solid model for rapid prototyping. *International Journal of Production Research*. 2000 Jan 10;38(1):69–83.
39. Fu G, Fu J, Lin Z, Shen H, Jin Y. A polygons Boolean operations-based adaptive slicing with sliced data for additive manufacturing. *Proceedings of the Institution of Mechanical Engineers, Part C: Journal of Mechanical Engineering Science*. 2017 Aug 24;231(15):2783–99.
40. Rianmora S, Koomsap P. Recommended slicing positions for adaptive direct slicing by image processing technique. *International Journal of Advanced Manufacturing Technology*. 2010 Feb 4;46(9–12):1021–33.
41. Kumar C, Choudhury AR. Volume deviation in direct slicing. *Rapid Prototyping Journal* [Internet]. 2005 [cited 2020 Aug 26];11(3):174–84. Available from: <https://www.emerald.com/insight/content/doi/10.1108/13552540510601309/full/html>
42. Taufik M, Jain PK. Volumetric error control in layered manufacturing. In: *Proceedings of the ASME Design Engineering Technical Conference* [Internet]. American Society of Mechanical Engineers (ASME); 2014 [cited 2020 Aug 25]. Available from: <http://asmedigitalcollection.asme.org/IDETC-CIE/proceedings-pdf/IDETC-CIE2014/46353/V004T06A017/4259083/v004t06a017-detc2014-35099.pdf>

43. Alexa M, Hildebrand K, Lefebvre S. Optimal discrete slicing. *ACM Transactions on Graphics* [Internet]. 2017 Jan 1 [cited 2021 Feb 4];36(1):1–16. Available from: <https://dl.acm.org/doi/10.1145/2999536>
44. Taufik M, Jain PK. Surface roughness improvement using volumetric error control through adaptive slicing. *Int J Rapid Manufacturing*. 2017;6(4):279–302.
45. Sikder S, Barari A, Kishawy HA. Global adaptive slicing of NURBS based sculptured surface for minimum texture error in rapid prototyping. *Rapid Prototyping Journal*. 2015 Oct 19;21(6):649–61.
46. Deng A, Badr Y, Gupta P. Dynamic programming approach to adaptive slicing for optimization under a global volumetric error constraint. In: Helvajian H, Piqué A, Gu B, editors. *Laser 3D Manufacturing V*. SPIE-Intl Soc Optical Eng; 2018. p. 11.
47. Wasserfall F, Hendrich N, Zhang J. Adaptive slicing for the FDM process revisited. In: *IEEE International Conference on Automation Science and Engineering*. IEEE Computer Society; 2017. p. 49–54.
48. Mueller CT, Irani A, Jenett BE. *Additive Manufacturing of Structural Prototypes for Conceptual Design*. 2014.
49. Tam KMM, Mueller CT. Additive Manufacturing Along Principal Stress Lines. *3D Printing and Additive Manufacturing*. 2017 Jun 1;4(2):63–81.
50. Li H, Wang T, Sun J, Yu Z. The adaptive slicing algorithm and its impact on the mechanical property and surface roughness of freeform extrusion parts. *Virtual and Physical Prototyping*. 2016 Jan 2;11(1):27–39.
51. Singamneni S, Roychoudhury A, Diegel O, Huang B. Modeling and evaluation of curved layer fused deposition. *Journal of Materials Processing Technology*. 2012 Jan 1;212(1):27–35.
52. Chen L, Chung MF, Tian Y, Joneja A, Tang K. Variable-depth curved layer fused deposition modeling of thin-shells. *Robotics and Computer-Integrated Manufacturing*. 2019 Jun 1;57:422–34.
53. Pelzer L, Hopmann C. Additive manufacturing of non-planar layers with variable layer height. *Additive Manufacturing*. 2021 Jan 1;37:101697.

54. Tam KMM, Mueller CT. Additive Manufacturing Along Principal Stress Lines. 3D Printing and Additive Manufacturing. 2017 Jun 1;4(2):63–81.
55. Chakraborty D, Aneesh Reddy B, Roy Choudhury A. Extruder path generation for Curved Layer Fused Deposition Modeling. CAD Computer Aided Design. 2008 Feb 1;40(2):235–43.
56. Sun Q, Rizvi GM, Bellehumeur CT, Gu P. Effect of processing conditions on the bonding quality of FDM polymer filaments. Rapid Prototyping Journal. 2008 Mar 28;14(2):72–80.
57. Mueller CT, Irani A, Jenett BE. Additive Manufacturing of Structural Prototypes for Conceptual Design. 2014.
58. Abbott AC, Tandon GP, Bradford RL, Koerner H, Baur JW. Process-structure-property effects on ABS bond strength in fused filament fabrication. Additive Manufacturing. 2018 Jan 1;19:29–38.
59. Thomas JP, Rodríguez JF. Modeling the Fracture Strength between Fused-Deposition Extruded Roads [Internet]. 2000 International Solid Freeform Fabrication Symposium. 2000 [cited 2020 Nov 19]. Available from: <https://repositories.lib.utexas.edu/handle/2152/74942>
60. Rosa F, Graziosi S. A parametric and adaptive slicing (PAS) technique: general method and experimental validation. Rapid Prototyping Journal. 2019 Jan 7;25(1):126–42.
61. Etienne J, Alexa M, Ray N, Panozzo D, Hornus S, L Wang CC, et al. CurviSlicer: Slightly curved slicing for 3-axis printers. ACM Trans Graph. 2019;38(4):11.
62. Isa MA, Lazoglu I. Five-axis additive manufacturing of freeform models through buildup of transition layers. Journal of Manufacturing Systems. 2019 Jan 1;50:69–80.
63. Dolenc A, Mäkelä I. Slicing procedures for layered manufacturing techniques. Computer-Aided Design. 1994 Feb 1;26(2):119–26.
64. O'Rourke J. Computational Geometry in C. 2nd ed. Computational Geometry in C. Cambridge: Cambridge University Press; 1998.

65. McLaurin D, Marcum D, Remotigue M, Blades E. Repairing unstructured triangular mesh intersections. *International Journal for Numerical Methods in Engineering*. 2013 Jan 20;93(3):266–75.
66. MATLAB. Working with Delaunay Triangulations - MATLAB & Simulink - MathWorks United Kingdom.
67. Krishnan Suresh. Volume of a surface triangulation . 2020.
68. Sylvain Lefebvre, Salim Perchy, Cédric Zanni, Pierre Bedell. IceSL Slicer. 2021.
69. slicing - How is E value calculated in Slic3r? - 3D Printing Stack Exchange [Internet]. 2019 [cited 2020 Dec 7]. Available from: <https://3dprinting.stackexchange.com/questions/10171/how-is-e-value-calculated-in-slic3r>
70. Boschetto A, Bottini L. Design for manufacturing of surfaces to improve accuracy in Fused Deposition Modeling. *Robotics and Computer-Integrated Manufacturing*. 2016 Feb 1;37:103–14.
71. Tronvoll SA, Elverum CW, Welo T. Dimensional accuracy of threads manufactured by fused deposition modeling. *Procedia Manufacturing*. 2018 Jan 1;26:763–73.
72. Turner BN, Gold SA. A review of melt extrusion additive manufacturing processes: II. Materials, dimensional accuracy, and surface roughness. *Rapid Prototyping Journal*. 2015 Apr 20;21(3):250–61.
73. Huang Q, Zhang J, Sabbaghi A, Dasgupta T. Optimal offline compensation of shape shrinkage for three-dimensional printing processes. <http://dx.doi.org/10.1080/0740817X2014955599> [Internet]. 2015 May 4 [cited 2021 Aug 11];47(5):431–41. Available from: <https://www.tandfonline.com/doi/abs/10.1080/0740817X.2014.955599>
74. Huang Z, Dantan JY, Etienne A, Rivette M, Bonnet N. Geometrical deviation identification and prediction method for additive manufacturing. *Rapid Prototyping Journal*. 2018 Nov 21;24(9):1524–38.
75. Dilberoglu UM, Simsek S, Yaman U. Shrinkage compensation approach proposed for ABS material in FDM process. <https://doi.org/10.1080/1042691420191594252>

- [Internet]. 2019 Jul 4 [cited 2021 Aug 11];34(9):993–8. Available from: <https://www.tandfonline.com/doi/abs/10.1080/10426914.2019.1594252>
76. Huang B, Singamneni SB. Curved layer adaptive slicing (CLAS) for fused deposition modelling. *Rapid Prototyping Journal*. 2015 Jun 15;21(4):354–67.
 77. Hebda M, McIlroy C, Whiteside B, Caton-Rose F, Coates P. A method for predicting geometric characteristics of polymer deposition during fused-filament-fabrication. *Additive Manufacturing*. 2019 May 1;27:99–108.
 78. Greeff GP, Schilling M. Closed loop control of slippage during filament transport in molten material extrusion. *Additive Manufacturing*. 2017 Mar 1;14:31–8.
 79. Oleff A, Küster B, Stonis M, Overmeyer L. Process monitoring for material extrusion additive manufacturing: a state-of-the-art review. *Progress in Additive Manufacturing* 2021 [Internet]. 2021 May 19 [cited 2021 Aug 5];1–26. Available from: <https://link.springer.com/article/10.1007/s40964-021-00192-4>
 80. Liu C, Law ACC, Roberson D, Kong Z (James). Image analysis-based closed loop quality control for additive manufacturing with fused filament fabrication. *Journal of Manufacturing Systems*. 2019 Apr 1;51:75–86.
 81. Mercado Rivera FJ, Rojas Arciniegas AJ. Additive manufacturing methods: techniques, materials, and closed-loop control applications. *The International Journal of Advanced Manufacturing Technology* 2020 109:1 [Internet]. 2020 Jun 29 [cited 2021 Aug 10];109(1):17–31. Available from: <https://link.springer.com/article/10.1007/s00170-020-05663-6>